A DISSERTATION

FOR THE DEGREE OF DOCTOR OF PHILOSOPHY

Bone Healing Effects of Osteogenic induced Mesenchymal Stromal Cell Sheets in Canine Fracture Models

개의 골절 모델에서 골분화를 유도한 중간엽 줄기세포 시트의 골재생 효과

by

Yongseok Yoon

MAJOR IN VETERINARY CLINICAL SCIENCES

DEPARTMENT OF VETERINARY MEDICINE

GRADUATE SCHOOL OF

SEOUL NATIONAL UNIVERSITY

August 2020

Bone Healing Effects of Osteogenic Induced Mesenchymal Stromal Cell Sheets in Canine Fracture Models

by

Yongseok Yoon

Supervised by Professor Byung-Jae Kang

A Dissertation submitted to

the Graduate School of Seoul National University

in partial fulfillment of the requirement

for the degree of Doctor of Philosophy in Veterinary Clinical Sciences

June 2020

Major in Veterinary Clinical Sciences

Department of Veterinary Medicine

Graduate School of

Seoul National University

August 2020

Bone Healing Effects of Osteogenic Induced Mesenchymal Stromal Cell Sheets in Canine Fracture Models

Advisor: Professor Byung-Jae Kang

Submitting a doctoral thesis of veterinary clinical sciences

June 2020

Graduate School of Seoul National University

Veterinary Clinical Sciences

Department of Veterinary Medicine

Yongseok Yoon

Confirming the doctoral thesis written by Yongseok Yoon

June 2020

Chair	Wan Hee Kim	_____
Vice Chair	Byung-Jae Kang	_____
Examiner	Oh-Kyeong Kweon	_____
Examiner	Min-Cheol Choi	_____
Examiner	Heung-Muong Woo	_____

Bone Healing Effects of Osteogenic Induced Mesenchymal Stromal Cell Sheets in Canine Fracture Models

Supervised by

professor Byung-Jae Kang

Yongseok Yoon

Major in Veterinary Clinical Sciences

Department of Veterinary Medicine

Graduate School of Seoul National University

ABSTRACT

Nonunion and delayed union during fracture repair are critical in veterinary orthopedic surgery. Mesenchymal stromal cells (MSC) sheets have potential for clinical application in bone regeneration. The bone regeneration capacity of

gelatin-induced osteogenic differentiated mesenchymal stromal cell sheets (GCS) was evaluated in this study. The effects were similar to those of osteogenic differentiated mesenchymal stromal cell sheets (OCS).

The study comprised two parts. First, OCS and undifferentiated mesenchymal stromal cell sheets (UCS) were compared for bone regeneration. Second, the efficacy of frozen and thawed GCS (FT-GCS) on the osteogenic potential of fresh GCS was assessed. Both parts of the study evaluated the bone healing capacity in canine model.

The first chapter compared the bone generation capacity of UCS and OCS *in vitro* and *in vivo*. Quantitative real-time polymerase chain reaction (rt-PCR) showed that runt-related transcription factor 2 (Runx2), bone morphogenetic protein 7 (BMP7) and hepatocyte growth factor (HGF) were upregulated in OCS compared to UCS. The expression levels of cyclooxygenase-2 (COX-2), interleukin-6 (IL-6), interleukin-10 (IL-10) and tumor necrosis factor - α (TNF-α) in UCS were markedly upregulated compared to OCS. *In vivo*, each stem cell sheet was applied in the radial fracture model. The proportions of external callus in the total bone volume of OCS group was significantly lower than that in the control. The OCS group showed significantly increased mature bone compared to the control and UCS groups. Fibrous connective tissue was increased in the UCS group. In OCS, the fracture sites could be stabilized by

early bone healing and callus formation was reduced, suggesting that UCSs and OCSs had different tissue healing effects and OCS could be used for bone healing.

The use of gelatin in the production of OCS increased bone differentiation-related factors, producing more solid OCS. In addition, the pathway of bone differentiation was different for OCS and GCS. Since it took several days to cultivate the OCS, the bone regeneration efficacy of the cell sheets was frozen and stored for easy evaluation of their clinical application.

In the second chapter, the bone regeneration effects of fresh GCS (F-GCS) and FT-GCS were evaluated. The experiment was performed in two parts. The first part involved *in vitro* evaluation of osteogenic potential of F-GCS and FT-GCS. The second part involved *in vivo* examination of the bone healing effects of both sheets in a canine model of fracture. *In vitro*, rt-PCR revealed no significant difference in the values of osteogenic-related factors between the two groups, and *in vivo* results, the external callus and the connectivity of fracture sites in both the F-GCS and FT-GCS groups were significantly increased compared to the control group. The amount of mature bones at fracture sites was increased in the F-GCS and FT-GCS groups compared to the control group, with no difference between the F-GCS and FT-GCS groups. Thus, bone regeneration using fresh and frozen-thawed GCS was similarly effective.

In conclusion, OCS can be clinically applied to promote early bone regeneration. In particular, OCS cultured with gelatin are more solid and osteogenic differentiated than OCS, even when frozen and stored, the bone regeneration effects of GCS could be expected.

―――

CONTENTS

CHAPTER I

Different Bone Healing Effects of Undifferentiated and Osteogenic Differentiated Mesenchymal Stromal Cell Sheets in Canine Radial Fracture Model

CHAPTER II

Frozen-thawed gelatin-induced osteogenic cell sheets of canine adipose-derived mesenchymal stromal cells improved fracture healing in canine model

LIST OF ABBREVIATIONS

A2-P	Ascorbic acid 2-phosphate
Ad-MSC	Adipose derived mesenchymal stromal cell
ARS	Alizarin red s
BMP7	Bone morphogenetic protein 7
COX-2	Cyclooxygenase-2
CT	Computed tomography
DMEM	Dulbeco's modified Eagle's medium
DMSO	Dimethyl sulfoxide
ECM	Extracellular matrix
F-GCS	Fresh gelatin-induced osteogenic differentiated mesenchymal stromal cell sheet
FT-GCS	Frozen thawed gelatin-induced osteogenic differentiated mesenchymal stromal cell sheet
GAPDH	Glyceraldehyde 3-phosphate dehydrogenase
GCS	Gelatin-induced osteogenic differentiated mesenchymal stromal cell sheet
HGF	Hepatocyte growth factor
H&E	Hematoxylin and eosin
IL-6	Interlukin-6
IL-10	Interlukin-10
MSC	Mesenchymal stromal cell
OCS	Osteogenic differentiated mesenchymal stromal cell sheet
OPN	Osteopontin
P/S	Penicillin/streptomycin
rt-PCR	Quantitative real-time polymerase chain reaction

Runx2	Runt-related transcription factor 2
TGF-β	Transforming growth factor -β
TNF-α	Tumor necrosis factor- α
UCS	Undifferentiated mesenchymal stromal cell sheet
u-MSC	Undifferentiated mesenchymal stromal cell

LIST OF FIGURES

x

LIST OF TABLES

GENERAL INTRODUCTION

MSCs have potential for differentiation to osteocytes, adipocytes and neurons (Parekkadan & Milwid, 2010; Uccelli, Moretta, & Pistoia, 2008). Therefore, MSCs are attractive tool in regenerative medicine, as they promote tissue repair by replacing damaged cells, inhibiting inflammation, and regulating growth factors (L. Chen, Tredget, Wu, & Wu, 2008; Huang, Xu, Zhang, Sun, & Li, 2015; Kassem & Abdallah, 2008).

Intravenously administered stem cells migrate to various organs, making it difficult to induce sufficient effects at the target site (Matsuura, Utoh, Nagase, & Okano, 2014), while tranplanted single-cell suspensions do not attach or proliferate in the target tissues. Therefore, the cell sheet morphology which can be applied locally at a specific site, has been considered. Cell sheets are appropriate for transplantation because of their cell-cell junction and abundant endogenous extracellular matrix. Indeed, cell sheets have been successfully used for regeneration in ligaments, liver, urinary bladder, heart, cornea and bone (Yang et al., 2007).

Cell sheets technology using temperature-responsive culture dishes (Matsuda et al., 2008; Uchiyama, Yamato, Sasaki, Okano, & Ogiuchi, 2006), using A2-P, or co-culturing with gelatin have been proposed, and the stemness and

transdifferentiation of cell sheets has been proven (A. Y. Kim et al., 2017; Lin et al., 2013; Wei et al., 2012; Yu, Tu, Tang, & Cheng, 2014).

Osteogenic differentiated MSCs have been used for bone regeneration and promotion of bone healing. OCSs have osteogenic potential (Akahane et al., 2008; Guo, Zeng, & Zhou, 2015; Ma et al., 2010; Wei et al., 2012) and OCSs have been studied for bone healing and promote bone regeneration *in vivo* (Inagaki et al., 2013).

Gelatin-induced osteogenic cells sheets can improve cellular proliferation and, extracellular matrix production, as well as significantly upregulate osteogenic markers compared to OCSs (A. Y. Kim et al., 2017).

In order to apply stem cells during fracture surgery, they can be used more conveniently if they are stored frozen. Some studies have showed that the continuous culture of stem cells results in chromosomal aberrations and autogenous malignant transformation (Froelich et al., 2013; Roemeling-van Rhijn et al., 2013). Therefore, cryopreservation of stem cells is an effective strategy. Other studies showed that cryopreservation of stem cells decreased the cells viability, differentiation capacity and reduce their homing ability, and fibronectin connection capacity (Chinnadurai et al., 2014; Pal, Hanwate, & Totey, 2008). Otherwise, some studies showed that frozen-thawed OCSs can

reportedly maintain their osteogenic potential and produce a highly mineralized matrix in bone defective sites (Kura et al., 2016).

In fracture patients, early bone union is very important to help the bone regeneration response by providing the stability of fracture. The purpose of this study is to develop a cell sheet that can help bone stability through rapid bone formation during the initial fracture recovery process. Besides, it is necessary to determine whether bone stability can be achieved even when cell sheets are frozen and stored before use. In the first experiment, the recovery process of bone regeneration was compared between OCS and UCS. The second experiment was conducted using GCS, which was found to have better bone differentiation ability than OCS. The bone resilience of F-GCS and FT-GCS were compared to evaluate whether a sufficient effect can be expected when using clinically stored cell sheets.

CHAPTER I

Different Bone Healing Effects of Undifferentiated and Osteogenic Differentiated Mesenchymal Stromal Cell Sheets in Canine Radial Fracture Model

ABSTRACT

   Cell sheets technology is now becoming available for fracture healing. This study evaluated bone healing effects of UCSs and OCSs in fracture model dogs. UCSs and OCSs were harvested at 10 days of culture. Transverse fractures at radius of six beagle dogs were assigned into UCS, OCS and control groups (n=4, in each group). The fractures were fixed with a 2.7 mm locking plate and six screws. Cell sheets were wrapped around fracture sites. Bones were harvested 8 weeks after operation, scanned by micro-CT and analyzed histopathologically. Additional two dogs were randomly divided to control, UCS and OCS group for evaluating early bone healing. Micro-CT revealed different aspects of bone

regeneration according to groups. At 8 weeks the percentages of external callus volume from total bone volume in the control, UCS, and OCS groups were 42.1%, 13.0% and 4.9% respectively ($p < 0.05$). Percentages of limbs with connectivity of gap were 25.0%, 12.5%, and 75.0%, respectively. In histopathological assessments, the OCS group at 4 weeks showed peripheral cartilage between the gap but other groups showed fibrous connective tissue. At 8 weeks the OCS group showed well organized and mature woven bone with peripheral cartilage at fracture sites, the control group showed cartilage formation without bone maturation or ossification at fracture site. Fracture sites were only filled with fibrous connective tissue without endochondral ossification and bone formation in the UCS group.

In OCS, early bone healing might stabilize the fracture site and lessened the callus formation. The results suggested that UCSs and OCSs had different tissue healing effect and OCSs could be used for bone healing.

INTRODUCTION

MSCs have potentials for bone regeneration (A.E. Rapp et al., 2015; Endrigo GL Alves et al., 2014; Huang et al., 2015). Previous report indicated that MSCs could repair damaged tissue by replacing damaged cells (Huang et al., 2015). Furthermore, MSCs may indirectly contribute to tissue repair through regulation of inflammation and secretion of cytokines (L. Chen et al., 2008; Kassem & Abdallah, 2008). Injection of suspended MSCs for delivery to target tissues has the disadvantage of MSCs disappearing from the system soon after transplantation (Matsuura et al., 2014). Cell sheets technology using temperature-responsive culture dishes (Matsuda et al., 2008; Uchiyama et al., 2006) or using A2-P has been proposed, and the stemness and transdifferentiation of cell sheets has been proven (Lin et al., 2013; Wei et al., 2012; Yu et al., 2014).

Cell sheets retain cell-cell junctions and are able to secrete abundant endogenous extracellular matrix (ECM) (Wei et al., 2012; Yu et al., 2014) and form multiple layers (Egami, Haraguchi, Shimizu, Yamato, & Okano, 2014). An intact cell sheet structure guarantees homeostasis of the cellular microenvironment during delivery of cytokines over a period of time to

accelerate tissue repair (Guo et al., 2015; Matsuura et al., 2014). Cell sheets have been evaluated in the regeneration of the ligament, cornea, urinary bladder, liver, heart and bone (Yang et al., 2007).

UCSs and OCSs have been used for bone regeneration, and both types of cell sheets have been reported to promote bone healing (Akahane et al., 2008; Akahane et al., 2010; Geng et al., 2013; Nakamura et al., 2010; Shimizu et al., 2015; Uchihara et al., 2015). OCSs cultured over 10 days can easily be folded away because of cellular aggregation, but UCSs could be cultured for longer (Guo et al., 2015; Kuk, Kim, Lee, Kim, & Kweon, 2015). Previous study showed that OCSs could produce more osteogenic-related factors than UCSs at 7 - 10 days after differentiation and this time was suitable for application at the fracture site (Kuk et al., 2015).

Pins have been used for internal fixation in studies in which the effects of cell sheets on bone regeneration were evaluated because more rigid fixation with plates and screws could not be applied in experimental animals such as mice, rats and rabbits (Akahane et al., 2008; Inagaki et al., 2013; Nakamura et al., 2010; Shimizu et al., 2015; Syed-Picard, Shah, Costello, & Sfeir, 2014; Uchihara et al., 2015; Wang et al., 2015). The bone healing pathway with unstable fixation is secondary bone healing with cartilaginous callus formation but not primary bone healing through intramembranous ossification (Tobias &

Johnston, 2012).

It may be suggested that the type of sheets and fixation method affect the bone healing pathway. This study was performed to clarify whether UCSs and OCSs under rigid fixation promote bone healing by different pathways.

MATERIALS AND METHODS

1. Isolation and culture of canine adipose tissue derived mesenchymal stromal cells

All animal experimental procedures were approved by the Institutional Animal Care and Use Committee of Seoul National University (SNU-150423-6). Canine ad-MSCs were obtained according to the methods described in previous paper (Ryu HH, 2009). In brief, fat tissues were harvested aseptically from the gluteal subcutaneous fat of beagle dogs. The tissues were washed with Dulbecco's phosphate-buffered saline (DPBS, Gibco, Grand Island, NY, USA), and immersed in collagenase type I (1 mg/ml; Sigma-Aldrich, St Louis, MO, USA) for 2 hours at 37 °C. After treatment with collagenase type 1, the samples were washed with phosphate-buffered saline (PBS) and centrifuged at $300 \times g$ for 10 minutes. The pellet was resuspended and filtered through a 100 µm nylon mesh. Those cells were seeded on the dishes and incubated in low-glucose Dulbeco's modified Eagle's medium (DMEM, HyClone, Logan, UT, USA) with 10% fetal bovine serum (FBS, Gibco BRL, Grand Island, NY, USA) and 1% penicillin/streptomycin (P/S, Hyclone) at 37 °C with 5% humidified CO_2.

The medium was changed every 2 days until the dishes became confluent with cells. After cells reached 90% confluency, they were subcultured.

2.　　Preparation of cell sheets

The cells at passage 3 were seeded on 100 mm dishes and cultured in low DMEM with FBS and P/S. The medium was changed to the differentiation medium when the confluency reached 90% which contains 1×10^6 cells. To prepare UCSs, the differentiation medium consisted of low DMEM, 10% FBS, 1% P/S and 50 µg/ml A2-P (Sigma-Aldrich). In the case of OCSs, the differentiation medium consisted of high DMEM, 10% FBS, 1% P/S, A2-P 50 µg/ml and 10^{-7} M dexamethasone (Dex, Sigma-Aldrich). The medium was changed every 2 days and at 10 days from differentiation, the cell sheets were washed twice with PBS and harvested. These harvested cell sheets were applied at the fracture site.

3.　　Real-time polymerase chain reaction (real-time PCR)

To compare the factors related to inflammation and osteogenicity at the mRNA level, undifferentiated MSCs (u-MSCs) were cultured as a control. In the case of u-MSCs, total RNA was extracted when the cells reached 90% confluency. In the case of UCSs and OCSs, total RNA was extracted when they reached 10 days of culture. Total RNA was isolated using a Hybrid-R RNA Extraction Kit (GeneAll, Seoul, Republic of Korea) and the RNA concentration were determined by measuring the light absorbance at 260 nm using ImplenNanoPhotometer (model 1443, Implen GmbH, Munich, Germany). One milligram of total RNA was used to synthesize cDNA with PrimeScript II First-strand cDNA Synthesis kit (Takara, Otsu, Japan). The cDNA obtained was then amplified via real-time PCR using an ABI Step One Plus Real-time PCR System (Applied Biosystems) and SYBR Premix EX Taq (Takara, Otsu, Japan). The primers used for real-time PCR are listed in Table 1, and GAPDH was used as the housekeeping gene. Genes related to inflammation, including interlukin-6 (IL-6), interlukin-10 (IL-10), cyclooxygenase-2 (COX-2), tumor necrosis factor- α (TNF-α) and hepatocyte growth factor (HGF), and factors related to osteogenicity, including runt-related transcription factor 2 (Runx2), bone morphogenetic protein 7 (BMP7), and transforming growth factor -β (TGF-β) were assessed by real-time PCR.

4.　　Induction of fracture and application of cell sheets

Eight male beagle dogs (age, 2 - 3 years, body weight 8.0 ± 0.5 kg) were used in the study. Animals were premedicated with 30 mg/kg cefazolin (Chong Kun Dang Pharmaceutical Co., Seoul Korea), 4 mg/kg tramadol (Samsung Pharmaceutical Co., Seoul, Korea) and 0.5 mg/kg famotidine (Dong-A ST, Seoul, Korea). They were pre-anesthetized with 3 mg/kg alfaxalone (Jurox Pty. Limited Co., Rutherford, Austalia) and intubated with an endotracheal tube and anesthesia was maintained with isoflurane (Choongwae Pharmaceutical Co., Seoul, Korea).

Transverse fractures were induced at the middle of both radiuses with an oscillating saw. Those fracture sites were fixed with 7 holes, a 2.7 mm locking plate (LP), and six locking screws. (BS.COREM Co., Korea) The limbs of six dogs were randomly classified into three groups (n = 4 for each group): UCS, OCS and no treatment (control). Three layers of cell sheets were applied to fill and surround the gap (Fig.1). Dogs were subjected to post-operative care for 7 days. The skin incision was dressed every day until recovery and 8 weeks after surgery the limbs were harvested. Additional two dogs were randomly divided to control, UCS and OCS group for evaluation of early bone healing. Limbs of two dogs were harvested at 4 weeks after surgery.

5. Radiographic examination and micro-computed tomography (micro-CT)

The radiographic examination was conducted before the operation and at the end of each week after the operation for 8 weeks. Then the dogs were euthanized and their bones were harvested. These samples were fixed in 10% neutral buffered formalin (Sigma-Aldrich, St Louis, MO, USA) and were scanned after careful dissection and removal of the plates using a micro-CT system (SKYSCAN 1172: HIGH RESOLUTION DESK-TOP MICRO-CT). Briefly, the samples were scanned using a protocol that utilizes high resolution X-ray energy settings of 85 KVP and 118 µA with a pixel size of 31.8 µm. Bone was considered at threshold 60 - 255. Quantification of bone volume and external callus was performed by the CTan software (Brucker micro-CT, version 1.14.4.1). Using 200 layers, measurements were taken of the volume 3.5 mm above and below the fracture.

In the sagittal plane of micro CT view, the connectivity was presented as percentages of the number of cortical bones connected by trabecular bones out of 8 bones each group.

6.   Histopathological and histomorphometry analysis

Segments of bone which were harvested at 4 weeks after surgery, including fracture sites were processed for histological analysis without decalcification. Samples were fixed in 10% neutral buffered formalin for 2 weeks and processed for resin embedding using a Technovit 7200 resin (Heaeus KULZER, Germany) and hardening with UV embedding system (KULZER EXAKT 520, Germany). Longitudinal sections were cut in the sagittal planes using EXAKT diamond cutting system (EXAKT 300 CP, Germany). The central longitudinal sections from each radius were ground to a thickness of 40 μm stained with hematoxylin and eosin (H&E).

Harvested bones, which were harvested at 8 weeks after surgery, were decalcified in 8% nitric acid, embedded in paraffin and sectioned at 4 μm for hematoxylin and eosin staining or 8 μm for Masson's trichrome staining. Samples were evaluated for the degree of formation of cartilage, bone and fibrotic tissues at the fracture site. The slide images were analyzed using ImageJ (version 1.37, National Institutes of Health, Bethesda, MD, USA)

7.   Statistical Analysis

Data for each test group were presented as mean ± standard deviation (SD). The IBM SPSS Statistics 23 statistical software was used to analyze the data (SPSS INC., Chicago, IL, USA). The difference between groups was analyzed using the Kruskal-Wallis test. The Mann-Whitney U test was used to confirm the differences between groups. A P value of < 0.05 was considered to be significant.

RESULTS

1.　　Real-time PCR

The TGF-β mRNA expression levels in UCS and OCS were significantly upregulated compared to u-MSCs ($p < 0.05$, Fig. 1.2. A). Runx2 and BMP7 expression in OCS were up-regulated compared to both u-MSCs and UCS ($p < 0.05$, Fig. 1.2. B, C). In UCS, expressions levels of COX-2, TNF-α, IL-6 and IL-10 were markedly upregulated compared to those in u-MSCs and OCS ($p < 0.05$, Fig. 1.2. D, E, F, G). HGF expression level in OCS was increased significantly than those in UCS and u-MSCs ($p < 0.05$, Fig. 1.2. H). UCS also had higher level of HGF than u-MSCs.

2.　　Radiographic changes

X-ray results showed that the implants were in proper position for the entire course of the experimental study period, i.e., 8 weeks. All the groups showed a

healing response. At 2 weeks, the control group showed an external callus, while at 8 weeks the callus size definitely increased (Fig. 1.3. A, B, C). In contrast, the UCS and OCS groups did not show abundant callus formation as seen in control group (Fig. 1.3. D-I).

3. Micro computed tomography and morphometric analysis

Micro-CT analysis showed a large bony callus in the control (Fig. 1.4. A). Compared to the control, the callus size was less in the UCS and OCS groups (Fig. 1.4. B, C). The percentages of external callus volume out of total bone volume were 42.1%, 13.0% and 4.9% in the control, UCS and OCS groups, respectively. Callus size was found to be significantly higher in the control groups than in cell sheets treated groups. ($p < 0.05$, Fig. 1.4. D) The percentages of limbs with gap connectivity were 25.0%, 12.5%, and 75.0% in the control, UCS and OCS groups, respectively. (Fig. 1.4. E)

4. Histopathology of fractured bone

At 4 weeks after bone injury, the OCS-treated group showed peripheral cartilage at the fracture site (Fig. 1.5. E, F). However, control and UCS-treated groups did not have bone healing sign at the fracture site (Fig. 1.5. A, B, C, D).

At 8 weeks after bone injury, the OCS-treated group showed well organized and mature woven bone with peripheral cartilage at the fracture sites (Fig. 1.6. G, H, I). The control group showed cartilage formation in the early phase of bone healing, but there was little bone maturation or ossification at the fracture site (Fig. 1.6. A, B, C). In the UCS-treated group, the fracture site was only filled with fibrous connective tissue without endochondral ossification and bone formation (Fig. 1.6. D, E, F).

Histomorphometric analysis of fracture sites showed that the percentage of mature bone in the OCS group (Fig. 1.6. J, $p < 0.05$), percentage of cartilage in the control group (Fig. 1.6. K, $p < 0.05$) and percentage of fibrous connective tissue in the UCS group (Fig. 1.6. L, $p < 0.05$) were significantly higher than those in each of the other groups.

Discussion

In the present study, although fracture sites were fixed with the same fixation system (locking plate and screws) bone healing responses were different between groups. At 8 weeks after surgery, cartilage, fibrous connective tissue and bone were found at fracture sites mainly in the control, UCS and OCS groups, respectively.

Abundant external callus was found in the control group compared to UCS and OCS groups. The control group showed secondary bone healing that induced external callus formation as seen on X-ray and micro-CT. Abundant callus formation in the control is probably due to periosteal reaction after surgical injury and micromotion of fracture site. Bone has periosteum in the surface which have three layers; osteoblast, cambium and fibrous layers from outer cortex (Dwek, 2010). Preexisted osteoblasts and osteogenic progenitor cells from vessels of cambium participate in formation of callus. Callus formation is also proportional to instability of the fracture (Aro HT & EY, 1993).

Gap healing, a type of primary bone healing characterized by formation of bone at the fracture gap following little secondary bone healing, occurs when the fixation is rigid and the interfragmentary gap is approximately 1 mm or less

(Tobias & Johnston, 2012). If considerable strain is applied, although the gap is less than 1 mm, it could induce micromotion so that abundant callus is formed. The OCS group showed gap healing with the formation of bone and less external callus despite the same fixation as in the control group. Increase in the expression level of BMP7 in OCSs indicated that the cells might be mature osteoblasts (Kuk et al., 2015; Vaes et al., 2002). Furthermore BMP7 factor secreted by mature osteoblasts could stimulate to mobilize osteogenic progenitor cells near the fracture site (Komori, 2005, 2006). The mature osteoblasts could produce bone in the intercortical gap (Akahane et al., 2008), which would confer stability at the fracture site. OCSs have immune modulatory factors as well as osteogenic factors (Gu et al., 2014). Less abundant callus formation in OCS group than the control suggested that immune modulatory factors might reduce the periosteal reaction to bone injury. The TGF-β mRNA expression levels in OCS group were significantly upregulated compared to u-MSCs. Although TGF-β is a pleiotropic cytokine with potent regulatory and inflammatory activity (Sanjabi, Zenewicz, Kamanaka, & Flavell, 2009) it might function as an anti-inflammatory cytokine for OCS derived bone healing. Moreover, HGF expression level in OCS group was increased. It was reported that HGF promoted osteogenic differentiation and was a necessary component for the establishment of osteoblast

mineralization (Aenlle, Curtis, Roos, & Howard, 2014). Therefore, the gap was filled with bone with the least external callus formation.

UCS group showed lesser callus formation and more connective fibrous tissue than the control group. UCS showed significantly higher level of inflammatory cytokines including COX-2, TNF-α, and IL-6 which might negatively affect bone formation. It has been reported that inflammatory cytokines including IL-6 and TNF-α activate osteoclast and osteoclastogenesis (Kudo et al., 2003; Melanie Timmen et al., 2014; Napimoga et al., 2015; Palmqvist, Persson, Conaway, & Lerner, 2002; Parekkadan & Milwid, 2010; Rifas & Weitzmann, 2009). It has also been reported that proinflammatory cytokines including TNF-α, inhibit osteogenic differentiation from stem cells (Lacey, Simmons, Graves, & Hamilton, 2009). Expression of IL-10 in UCS group was elevated than other groups. IL-10 has immune modulatory effect (Sabat et al., 2010). Immune modulatory effect of IL-10 and inflammatory effect of proinflammatory cytokines delayed bone healing with less callus formation. It was reported that COX-2 and IL-6 expression was significantly higher in freeze–thawed cells than fresh MSCs and that these increases might be due to heat stress during the thawing process (M. Kim et al., 2016). Culture in the cell matrix for 10 days without differentiation seemed to induce stress in

MSCs. Further studies on the *in vivo* effects of increases in proinflammatory cytokines in UCSs are needed.

On the basis of these results, the difference in the osteogenic ability of OCSs and other groups might be due to early bone formation between the fracture gaps which stabilize the fracture site and result in less callus formation. It is suggested that OCSs and UCSs have different *in vivo* osteogenic abilities in fracture repair; that is, direct healing for OCSs and delayed healing for UCSs.

Table 1. 1. Primers used for real-time polymerase chain reaction

Primer		Primer sequence (5' – 3')
GAPDH	Forward	CATTGCCCTCAATGACCACT
	Reverse	TCCTTGGAGGCCATGTAGAC
BMP7	Forward	TCGTGGAGCATGACAAAGAG
	Reverse	GCTCCCGAATGTAGTCCTTG
Runx2	Forward	TGTCATGGCGGGTAACGAT
	Reverse	TCCGGCCCACAAATCTCA
TGF-β	Forward	CTCAGTGCCCACTGTTCCTG
	Reverse	TCCGTGGAGCTGAAGCAGTA
IL-10	Forward	CCTGGGAGAGAAGCTCAAGA
	Reverse	TGTTCTCCAGCACGTTTCAG
IL-6	Forward	TTTTCTGCCAGTGCCTCTTT
	Reverse	GGCTACTGCTTTCCCTACCC
COX-2	Forward	ACCCGCCATTATCCTAATCC
	Reverse	TCGGAGTTCTCCTGGCTTTA
TNF-α	Forward	ACCACACTCTTCTGCCTGCT
	Reverse	TGGAGCTGACAGACAACCAG
HGF	Forward	CTTGCAGTGTTTATGGCTGG
	Reverse	ATCCACGACCAGGAACAATG

Figure. 1.1. Implantation of cell sheets

Radiuses were fixed with 7hole Locking Plate. In UCS and OCS groups, cell sheets were applied to fill and surround the gap. Black arrow indicates cell sheets.
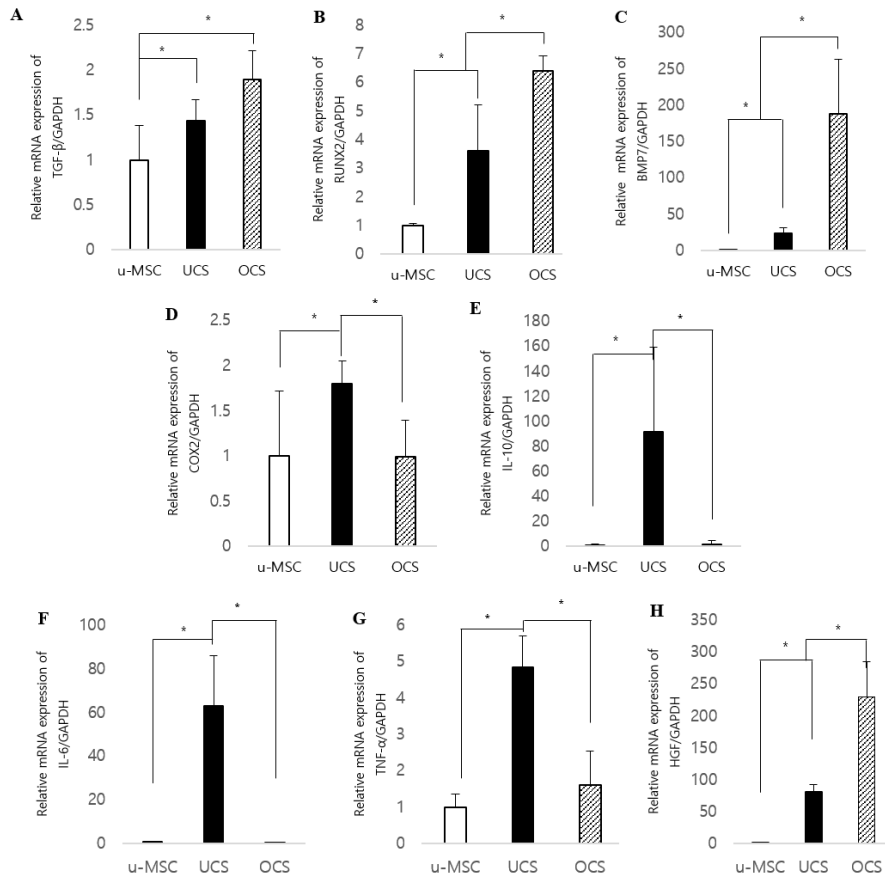
Figure 1.2. Osteogenic differentiation and inflammatory–related gene expression profiles of u-MSC, UCS and OCS at 10 days of culture.

The expressions of TGF-β mRNA in UCS and OCS groups were considerably upregulated compared to the u-MSC (A). Runx2 and BMP7 were up-regulated in OCS compared to both u-MSC and UCS (B, C). Expressions of COX-2, IL-6, IL-10 and TNF-α in UCS were markedly upregulated compared to u-MSC and OCS (D, E, F, G). In case of HGF, both groups showed upregulated compare to control (H). Each bar represents the mean ± SD. * represents statistically significant difference ($p < 0.05$).
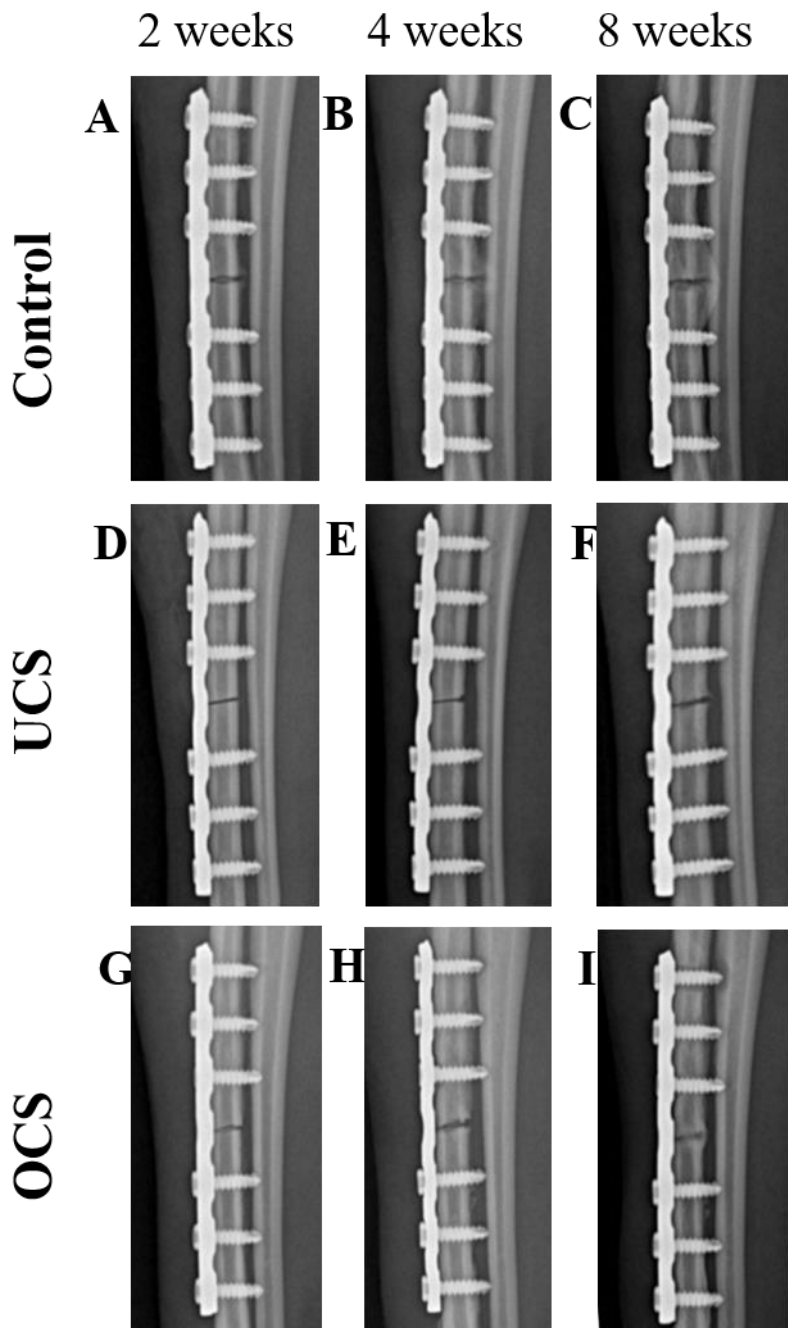
Figure 1.3. Radiographic changes of bone healing in relation to weeks.

Control group at 2 weeks showed external callus (A) but other groups did not (D, G). External callus in control group became larger (B) but osteolysis was observed in UCS group (E). The callus at 8 weeks was larger than at 4 weeks in control group (C). But in UCS and OCS groups, external callus was not observed as much as control group (F, I) and OCS group at 8weeks showed connectivity between the gap (I).
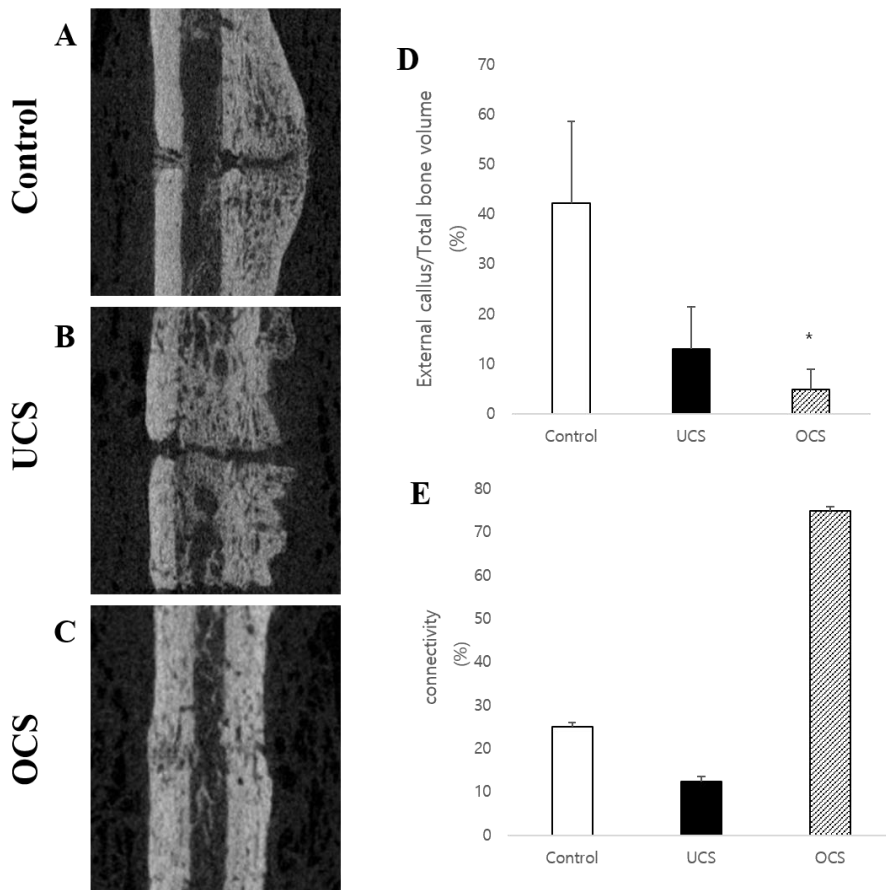
Figure 1.4. Micro-CT images at fracture sites and morphologic analysis of bone healing.

  Large bony callus formation was observed in the control but connectivity between cortical bones was not observed. (A) UCS and OCS groups showed no significant callus formation (B, C). In OCS group, there was connectivity between cortices, and the gaps were filled with materials which were similar attenuation as normal bone (C). The percentages of external callus volume out

of total bone volume in OCS group significantly decreased compare to the control (D). The percentages of cortical bones which had connectivity between corties were 25%, 12.5%, and 75% respectively (E).

4 weeks

A — Control
B

C — UCS
D
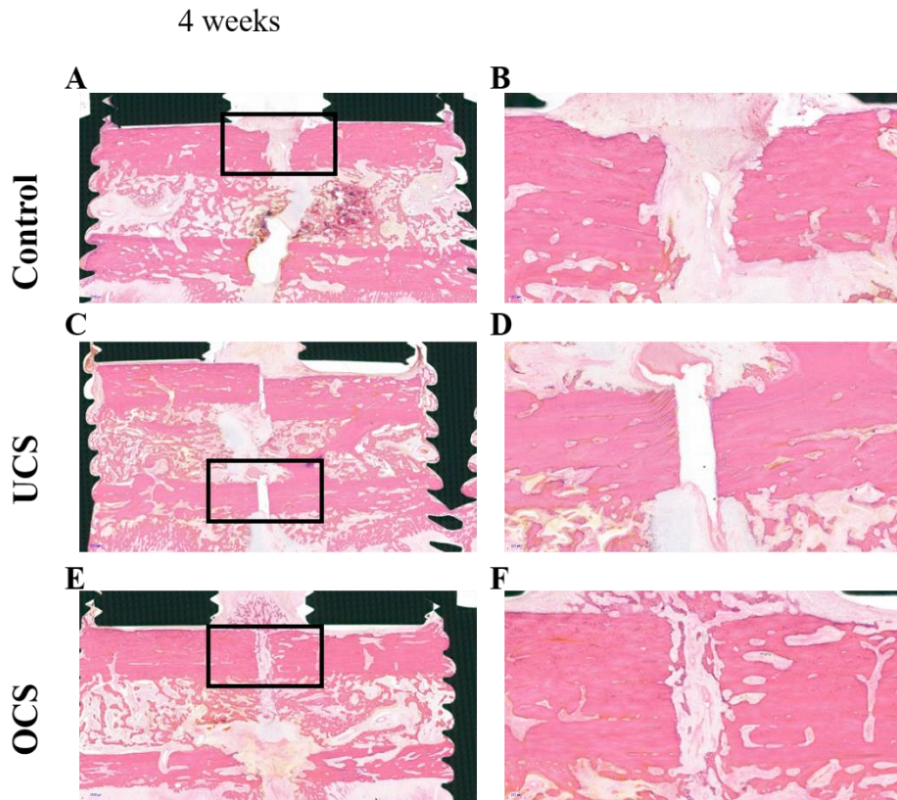
E — OCS
F

Figure 1.5. H&E staining. Histopathological findings of fracture sites at 4 weeks without decalcification

The OCS-treated group showed peripheral cartilage at the fracture site (E, F) at 4 weeks. However, control and UCS-treated groups did not have bone healing sign at the fracture site (A, B, C, D).
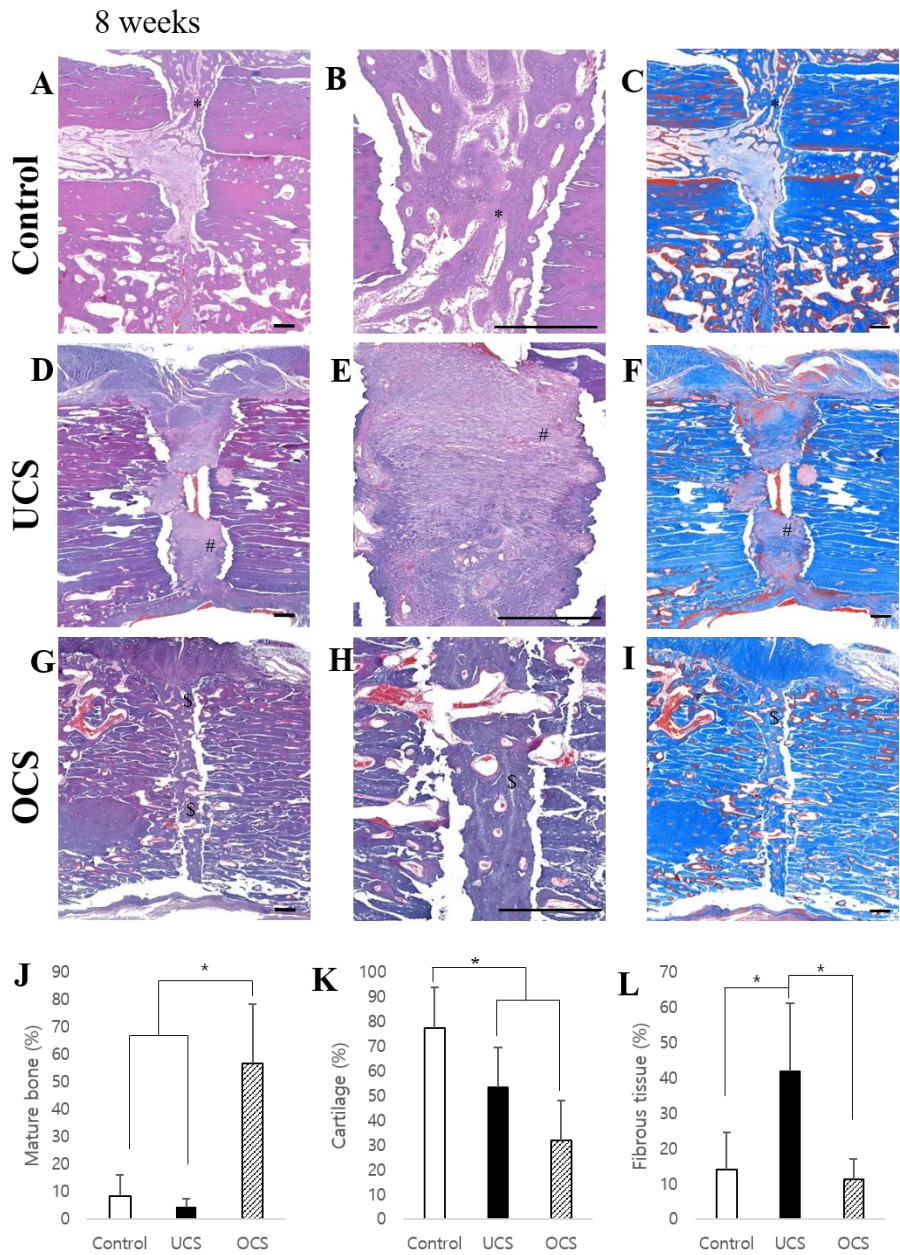
Figure 1.6. H&E staining, Masson's trichrome staining. Histopathological findings and histomorphometric analysis of fracture sites at 8 weeks post

cell sheets grafting

Control group showed cartilage formation (*) without ossification at fracture site. UCS group showed that the fracture site was filled with fibrous connective tissue (#) with less endochondral ossification or bone formation. OCS group showed that the fracture site was well organized with peripheral cartilage and mature woven bone. Scale bar: 100 µm.

OCS group showed significant increased mature bone compare to control and UCS group (J). Control group showed definitely increased cartilage compare to OCS (K). Fibrous connective tissue was increased in UCS group (L). Each bar represents the mean ± SD. * represent a statistically significant difference ($p < 0.05$).

CHAPTER II

Frozen-thawed gelatin-induced osteogenic cell sheets of canine adipose-derived mesenchymal stromal cells improved fracture healing in canine model

ABSTRACT

I assessed the efficacy of frozen-thawed gelatin-induced osteogenic cell sheet (FT-GCS) compared to that of fresh gelatin-induced osteogenic cell sheet (F-GCS) with adipose derived mesenchymal stromal cells (Ad-MSCs) used as the control. The bone differentiation capacity of GCS has already been studied. On that basis, the experiment was conducted to determine ease of use of GCS in the clinic. *In vitro*, there was no significant difference in mRNA expressions of Runx2, β-catenin, OPN, and BMP7 between F-GCS and FT-GCS. In an *in vivo* experiment, both legs of six dogs with transverse radial fractures were randomly assigned to one of three groups: F-GCS, FT-GCS, or control. Fracture sites were wrapped with the respective cell sheets and fixed with 2.7 mm

locking plates and six screws. At 8 weeks after the operations, bone samples were collected and subjected to micro computed tomography and histopathological examination. External volumes of callus as a portion of the total bone volume in control, F-GCS, and FT-GCS groups were 49.6%, 45.3%, and 41.9%, respectively. The histopathological assessment showed that both F-GCS and FT-GCS groups exhibited significantly ($p < 0.05$) well-organized, mature bone with peripheral cartilage at the fracture site compared to that of the control group. Based on my results, I infer that the cryopreservation process did not significantly affect the osteogenic ability of gelatin-induced cell sheets

INTRODUCTION

Mesenchymal stem cells can differentiate in osteocytes, adipocytes, and neurons. Therefore, they are a good source of regenerative medicine (Parekkadan & Milwid, 2010; Uccelli et al., 2008). Injected mesenchymal stem cells can migrate to various tissues owing to their homing capacity (Devine, Cobbs, Jennings, Bartholomew, & Hoffman, 2003). Nevertheless, shape, size, and position of the injected stem cells are difficult to control. Recently, sheets of stem cells have been developed to enhance cellular viability and to enhance local effects of transplanted stem cells (Kelm & Fussenegger, 2010). Other *in vitro* studies have shown that osteogenic-differentiated stem cell sheet (OCSs) have osteogenic potential (Akahane et al., 2008; Guo et al., 2015; Kuk et al., 2015; Ma et al., 2010; Wei et al., 2012). Additionally, *in vivo* application of OCSs promotes bone repair (Inagaki et al., 2013; Pirraco et al., 2011; Uchiyama et al., 2011; Yoon et al., 2017). Previously, it had shown that gelatin-induced osteogenic cells sheets (GCSs) have improved cellular proliferation, an ample amount of extracellular matrix production, and significant upregulation of osteogenic markers compared to those of OCSs (A. Y. Kim et al., 2017). However, the *in vivo* effects of fresh and frozen-thawed gelatin-induced osteogenic cell sheets (F-GCSs and FT-GCSs, respectively) remain unclear.

3 5

Other studies have illustrated that the continuous culture of stem cells results in chromosomal aberrations and spontaneous malignant transformations (Froelich et al., 2013; Roemeling-van Rhijn et al., 2013). Therefore, cryopreservation of stem cells is deemed inevitable. Moreover, at present, cryopreserved stem cells or sheets are more readily available than freshly cultured stem cells (Bruder, Jaiswal, & Haynesworth, 1997; Spurr, Wiggins, Marsden, Lowenthal, & Ragg, 2002). However, cryopreservation has its limitations as it already has been reported that cryopreservation of stem cells decreases the cells' viability, differentiation capacity, and reduces their homing ability, bio-distribution properties, and fibronectin connection capacity (Chinnadurai et al., 2014; Pal et al., 2008). Contrary to the application of stem cells, stem cell sheets can be applied regionally to provide an improved localized effect (Inagaki et al., 2013; Uchiyama et al., 2011; Yoon et al., 2017). Also, frozen-thawed OCSs can maintain their osteogenic potential and produce a highly mineralized matrix in bone defective sites (Kura et al., 2016).

Previously, it was reported that GCSs are significantly better than OCSs in terms of cell proliferation, extracellular matrix (ECM) formation, and upregulation of bone markers (A. Y. Kim et al., 2017). For the present study, I hypothesized that cryopreservation not only reduces cell sheet preparation time but also do not affect the osteogenic potential of GCSs. Thus, efficacy of FT-

GCSs to that of F-GCSs was compared. In addition, bone healing capacity of

both F-GCSs and FT-GCSs were evaluated in canine fracture model.

MATERIALS AND METHODS

1. Isolation and culture of canine Ad-MSCs

All experiments were approved by the Institute of Animal Care and Use Committee of Seoul National University (SNU-170203-2), South Korea. In addition, all experiments were carried out in accordance with the National Institute of Health guide for the care and use of Laboratory Animals (NIH Publication No. 8023, revised 1987).

Adipose-derived mesenchymal stromal cells (Ad-MSCs) were isolated as reported previously (Ryu HH, 2009). Briefly, Ad-MSCs were isolated aseptically from gluteal adipose tissue of 2-year-old male beagle dogs. Harvested adipose tissues were washed with Dulbecco's phosphate-buffered saline (DPBS; Gibco; Fisher Scientific USA) and immersed in 1 mg/mL collagenase type I (Sigma-Aldrich, USA) at 37 °C for 2 h. After treatment, the samples were washed with DPBS followed by centrifuging at 4 °C and $980 \times g$ for 10 min. The pellets of the stromal vascular fraction were resuspended, filtered through 100 μm nylon mesh, then incubated overnight in low-glucose Dulbecco's modified Eagle's medium (DMEM; HyClone, USA) supplemented

with 10% fetal bovine serum (FBS; Gibco BRL; Fisher Scientific) and penicillin and streptomycin (PS, 10,000 U/mL, Gibco; Fisher Scientific) at 37 °C in a humidified atmosphere containing 5% CO_2. After 24 h, the samples were washed with PBS to remove residual red blood and unattached cells. The medium was changed every 2 days, and the cells were sub-cultured to 90% confluence. Ad-MSCs at the third passage were used for subsequent experiments.

2. Preparation of fresh gelatin-induced osteogenic cells sheets (F-GCS)

F-GCSs were prepared in accordance with the method reported by Kim et al. (A. Y. Kim et al., 2017). Briefly, Ad-MSCs (5×10^5 cells) in the 3rd passage were seeded in 100 mm dishes or to 6-well plates per experimental requirements. Ad-MSCs were cultured in basal medium, low-glucose DMEM with 10% FBS (Gibco BRL; Fisher Scientific) and 1% penicillin and streptomycin (PS, 10,000 U/mL, Gibco; Fisher Scientific). When the seeded cells reached 60% –70% confluence, the basal medium was replaced with high-glucose DMEM with 10% FBS, 1% PS, 15 μg/mL L-ascorbic acid 2-phosphate (Sigma-Aldrich, USA), 10 mM β-glycerophosphate (SigmaAldrich), 0.1 μM dexamethasone (Sigma-Aldrich) and 0.02 g/mL gelatin powder

(SigmaAldrich). The gelatin-containing differentiation medium was changed after every two days. The GCSs were harvested on the 10th day of differentiation.

3. Cryopreservation of GCS (FT-GCS)

Frozen-thawed GCSs (FT-GCSs) were prepared using 3rd passage GCSs and the previously described slow-freezing method (Kura et al., 2016). After 10 days of differentiation in gelatin-containing differentiation medium, cell sheets were collected with the help of a cell scraper and transferred to 2 mL cryovials (cryogenic vial; BD Falcon). Each cryovial contained 500 μL FBS, 400 μL low-glucose DMEM, and 100 μL of dimethyl sulfoxide (DMSO). Cryovials containing GCSs were cryopreserved in a freezing container (NALGENE Cryo 1 °C Freezing Container; Sigma Aldrich, USA). Container temperature was slowly decreased (1°C/min) from 4 °C to − 180 °C. After 24 h, the samples were moved to a tank of liquid nitrogen. One week later, FT-GCSs were thawed in a water bath at 37 °C. The thawed FT-GCSs were washed twice with DPBS and then used for further experimentation.

4. Real-time polymerase chain reaction

  Isolation of mRNA was carried out by using a Hybrid-R RNA Extraction Kit (GeneAll, Korea). Complementary DNA was prepared by using a PrimeScript II First-strand cDNA Synthesis kit (Takara, Japan). An ABI Prism 7000 Sequence Detection System (Applied Biosystems, USA) was used to amplify the desired DNA. Green Mix (Enzo Life Science, USA) was used to detect gene expressions. Normalization was done with the help of glyceraldehyde-3-phosphate dehydrogenase (GAPDH) and was quantified by using the $\Delta\Delta Ct$ method (Livak & Schmittgen, 2001). All data were compared with that of fresh Ad-MSCs, which were used as the control. The primer sequences of target genes, runt-related transcription factor 2 (Runx2), β-catenin, osteopontin (OPN), Bone morphogenetic protein 7 (BMP7), and housekeeping gene GAPDH are shown in Table 1.

5. Capacity of mineralization

Mineralization of F-GCSs and FT-GCSs was measured on days 0, 5, and 11 of culture in gelatin-based basal media. Cell sheets were harvested and washed twice with DPBS before further processing. Afterward, cell sheets were fixed in 70% ethanol for 1 h at 25 °C, followed by washing with distilled water, staining with 2% Alizarin red stain (ARS; pH 4.2), and incubation for 20 min with shaking. After aspiration of the dye, samples were washed thoroughly with distilled water, after which, 1 mL of 10 mM (10%) cetylpyridinium chloride was added and the plates incubated for 60 min with shaking. Finally, 200 μL aliquots of the sample solution were transferred to a 96-well plate to read absorbance at 550 nm (Gregory, Gunn, Peister, & Prockop, 2004).

6. In vivo experiment

For fracture induction and cell sheet application, six male beagle dogs, 2 – 3 years of age with a body weight of 8.0 ± 0.5 kg, were used in the *in vivo* study. Pre-medication of the animals was done by applying 30 mg/kg of cefazolin (Chong Kun Dang Pharmaceutical, Korea), 0.5 mg/kg famotidine (Dong-A ST, Korea), and 4 mg/kg tramadol (Samsung Pharmaceutical, Korea) before manipulation. Alfaxalone (Jurox Pty. Limited, Australia; 3 mg/kg) was used for

pre-anesthetization, and intubation was carried out with an endotracheal tube. Anesthesia was maintained with isoflurane (Choongwae Pharmaceutical, Korea).

The radius bone of both right and left legs were subjected to induction of transverse fracture at the middle of the bone with an oscillation saw. The fractures were then fixed by applying a 7-hole 2.7 mm locking plate with six locking screws (BS. COREM Co., Korea). The 12 limbs of the six study dogs were randomly assigned to three groups (n = 4 per group): F-GCSs group, FT-GCSs group, and no treatment group (control). Three layers of respective cell sheets were applied to each limb to wrap the fracture site. Post-operative care of the dogs was carried out for seven days. All radius bones were harvested at 8 weeks after surgery for further analysis.

Radiographic and micro computed tomography examination was carried out before the operation and every week after the operation for 8 weeks. Afterward, dogs were euthanized and radius bones were harvested. The bones were then fixed with 10% neutral buffered formalin (Sigma-Aldrich, USA). The prepared bones were scanned using a micro-CT system (SKYSCAN 1172: High-Resolution Desk-top Micro-CT, Bruker, USA). Briefly, scanning was conducted using high-resolution X-ray energy settings of 85 KVP and 118 µA with a pixel size of 31.8 µm. Bone was considered present at a threshold of 60

- 255. CTAN software (Brucker micro-CT, version 1.14.4.1; Bruker) was used to quantify bone volume and external callus amount. Using 200 layers, volume measurements were taken at 3.5 mm above and below the fracture area.

In the sagittal plane of micro CT view, the connectivity was presented as percentages of the number of cortical bones connected by trabecular bones out of 8 bones each group.

Histopathological and histomorphometric analysis Harvested bones, at 8th week after surgery, were subjected for decalcification in 8% nitric acid and then embedded in paraffin for sectioning. Longitudinal sections were cut along a sagittal plane. Sections (4 µm thick) were used for H&E staining while 5 µm thick sections were used for Masson's trichrome staining. Stained samples were analyzed for cartilage and bone tissue formation at the fracture site. Analysis was carried out with the help of Image J (Version 1.37, National Institutes of Health, USA).

7. Statistical analysis

Data are presented as mean ± standard deviation values. The IBM software SPSS Statistics 23 (SPSS Inc., USA) was used for the data analysis. Difference

between groups was analyzed by applying the Kruskal-Wallis test. The Mann-Whitney U test was used as a post-hoc test. A p value of less than 0.05 was considered as indicative of a significant difference. *In vitro* experiments were repeated thrice.

RESULTS

Upregulation of osteogenic markers

Compared to the expression levels in Ad-MSCs, the F-GCSs and FT-GCSs both showed significant ($p < 0.05$) upregulation of Runx2, β-catenin, OPN and BMP7. However, there was no significant ($p < 0.05$) difference in the expressions of osteogenic genes between F-GCSs and FT-GCSs (Fig. 2.1. A-D).

Degree of mineralization

Mineralization analysis showed that even after cryopreservation the FT-GCSs exhibited a significant increase in their mineralization capacity. The absorbance of ARS by F-GCSs and FT-GCSs was significantly ($p < 0.05$) higher on days 5 and 11 than on day 0 (Fig. 2.2. B).

Radiographic and micro-CT imaging

Radiographic examination showed that implants retained their position for the entire 8 weeks after surgery (Fig. 2.3. A-I). Groups showed no significant

difference in healing at 1 week after surgery (Fig. 2.3. A, D, and G). After 4 weeks of healing, all groups showed the formation of external calluses (Fig. 2.3. B, E, and H), which increased in size after 8 weeks of healing (Fig. 2.3. C, F, and I). Formation of large bony calluses occurred in all groups (Fig. 2.3. a-c). Percentages of external callus volume out of the total bone volume for the control, F-GCSs, and FT-GCSs groups were 49.6% $\pm$ 1.05, 45.3% $\pm$ 4.08, and 41.9% $\pm$ 3.50, respectively. There was no significant difference in callus size among the groups (Fig. 2.3. d). The percentages of connectivity of cortices in each group were 21% in control, 81% in F-GCSs, and 80% in FT-GCSs ($p <$ 0.05, Fig. 2.3. e).

Histopathology of the fracture area

Histopathological analysis of harvested bones that were treated with F-GCSs and FT-GCSs revealed the presence of organized and mature bone with less peripheral cartilage on the fracture sites at 8 weeks after surgery (Fig. 2.4. D-I). However, there was formation of cartilage with little ossification at the fracture site in the control group limbs (Fig. 2.4. A-C).

Bone histomorphometric analysis of the groups treated with F-GCSs and FT-GCSs revealed significantly ($p <$ 0.05) greater presences of mature bone compared to that in the control group (Fig. 2.4. K). Moreover, the percentage

of cartilage formation in the control group was significantly ($p < 0.05$) higher

than those in the F-GCSs and FT-GCSs groups (Fig. 2.4. J).

DISCUSSION

Currently, performing bone reconstruction with tissue-engineered bone or an osteogenic cell sheet (OCS) is a lengthy procedure, which involves cell isolation, seeding, culturing, differentiation, and scaffold construction (Okamoto et al., 2006; Yoon et al., 2017). Therefore, bone fracture surgeries must be planned to coincide with cell preparation time. Hence, protocols for cell sheet or scaffold preparation may not be convenient for clinical therapies. Clinically, there is a need for a method which can reduce cell preparation time and increase the osteogenic potential of cells. Previously, it reported that the use of F-GCSs was significantly better in terms of proliferation, ECM production, and osteogenic bone marker production than those of OCSs (A. Y. Kim et al., 2017). However, F-GCSs also need preparation before administration, which can delay treatment of a bone fracture. Consequently, FT-GCSs was a suggested solution to that problem, as it showed good potential for mineralization and mature bone production. In addition, the immediate application of thawed FT-GCSs made its use more desirable and convenient than the use of F-GCSs or fresh-OCSs when supporting the healing of fractured bones.

Some authors have reported that cryopreservation of MSCs does not affect their osteogenic differentiation (Kotobuki et al., 2005). However, DMSO is reported to have cytotoxic effects and induces differentiation of MSCs into neuron-like cells (Chu, Wang, Fu, & Zhang, 2004) or cardiac myocytes (Young et al., 2004). My study results, showing no significant difference in the osteogenic differentiation and mineralization of FT-GCSs as compared to F-GCSs, support those studies that have reported that cryopreservation of stem cells sheets with DMSO does not alter mineralization or bone production capacity (Shimizu et al., 2013). These results were also supported by our real-time PCR results, which showed that expression levels of Runx2, OPN and BMP7 of FT-GCSs remained almost equal to those of F-GCSs. Runx2 is an important indicator of early osteogenic differentiation, while OPN and BMP7 are produced from mature osteoblasts in later stages of osteogenesis (G. Chen, Deng, & Li, 2012; Komori, 2005). Therefore, the results indicate GCSs differentiate into mature osteoblasts, and neither freezing-thawing nor DMSO has a significant negative effect on the osteogenic differentiation capacity of GCSs. Alizarin red stain (ARS) results showed that mineralization of FT-GCSs was significantly increased in the 5th and 11th day as compared to that on the 0th day of reculturing, suggesting that the osteogenic differentiation process, which was suspended as a result of cryopreservation, proceed continuously after thawing.

Various studies have reported the formation of a callus at the fracture site, even in the presence of strict fixation (Nakamura et al., 2010; Shimizu et al., 2015; Yoon et al., 2017). In this study, callus formation was observed in the control, F-GCSs, and FT-GCSs groups. This could be the result of secondary healing of the bones. Micro-motions and periosteal reaction could also have an effect on callus formation in all groups. Regardless, the F-GCSs and FT-GCSs groups had better healing capacities than the control group. Despite the same nature of fixation as that applied in the control group, there was a more formation of mature bone in F-GCSs and FT-GCSs groups. In addition, there was no significant difference in BMP7 expression between FT-GCSs and F-GCSs, which might be involved in the high level of mature bone production, less connective tissue formation, and fast healing time of fractures in the F-GCSs and FT-GCSs groups (Komori, 2005, 2006).

Injected stem cells can resettle to a specific tissue owing to their homing characteristics (Devine et al., 2003) However, cryopreservation has been reported to have a negative effect on homing characteristics of stem cells (Chinnadurai et al., 2014), reducing the homing ability of stem cells. However, cell sheets can be used in a localized area, therefore, cell sheets can be used more efficiently than stem cells (Kura et al., 2016). Moreover, gelatin contains an arginine-glycine-aspartic acid sequence, which promotes cells stability with

ECM (Hoch, Schuh, Hirth, Tovar, & Borchers, 2012) and cell adhesion through integrin (Rosellini, Cristallini, Barbani, Vozzi, & Giusti, 2009; Wu et al., 2011).

It is concluded that freezing and thawing did not affect the osteogenic ability of GCSs. Moreover, FT-GCSs can be utilized immediately after thawing with the same effects as those produced by F-GCSs.

Therefore, compared to F-GCSs, the use of FT-GCSs for fracture healing is more convenient.

Table. 2. 1. Primers used for real-time polymerase chain reaction

| Primer		Primer sequence (5' – 3')
GAPDH	Forward	CATTGCCCTCAATGACCACT
	Reverse	TCCTTGGAGGCCATGTAGAC
Runx2	Forward	TGTCATGGCGGGTAACGAT
	Reverse	TCCGGCCCACAAATCTCA
β-catenin	Forward	TACTGAGCCTGCCATCTGTG
	Reverse	TACTGAGCCTGCCATCTGTG
OPN	Forward	GATGATGGAGACGATGTGGATA
	Reverse	TGGAATGTCAGTGGGAAAATC
BMP7	Forward	TCGTGGAGCATGACAAAGAG
	Reverse	GCTCCCGAATGTAGTCCTTG
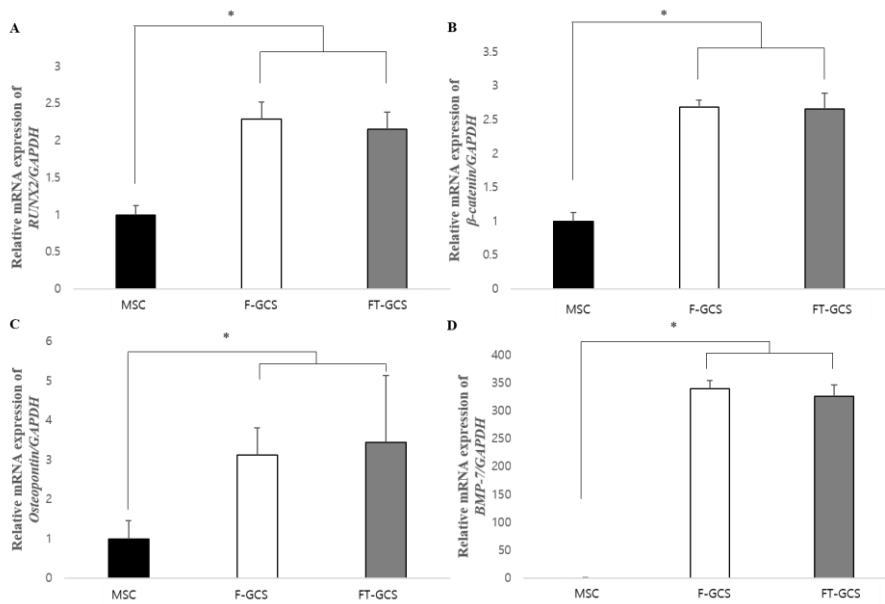
Fig. 2. 1. Expression of osteogenic makers of adipose-derived mesenchymal stromal cells, F-GCSs and FT-GCSs.

The mRNA expressions are relative to that of GAPDH and were evaluated by using quantitative real-time PCR for (A) Runx2, (B) β-catenin, (C) OPN, and (D) BMP7. Each bar indicates mean ± standard deviation; n = 3. * $p < 0.05$, significant difference from the control.
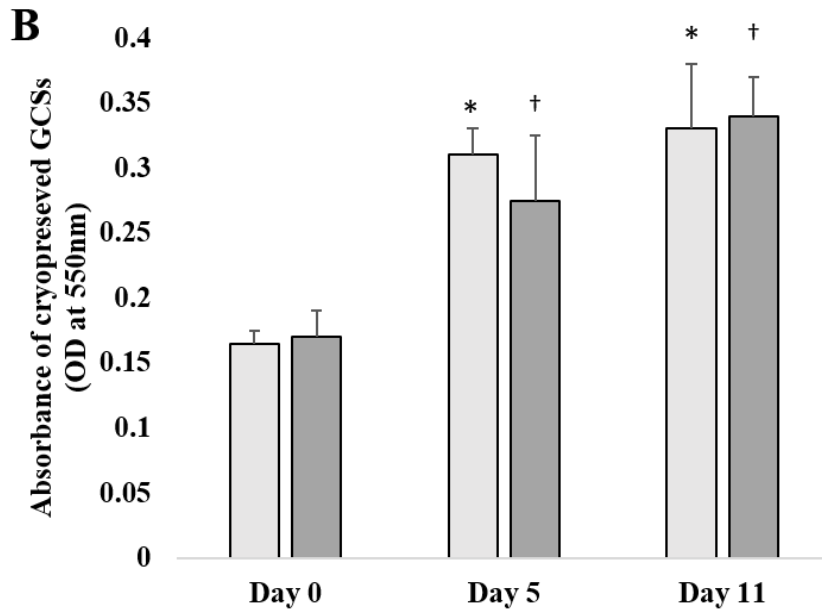
5 4

F-GCS   FT-GCS

A

Day 0

Day 5

Day 11

100 µm
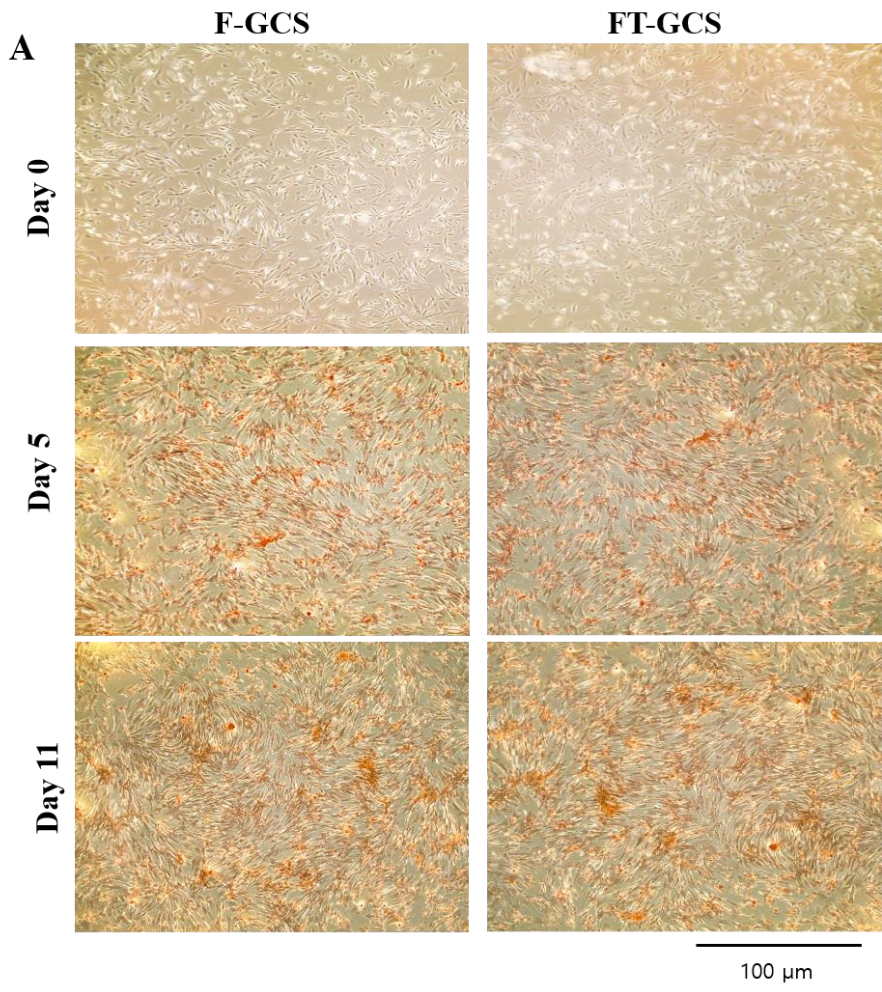
Fig. 2. 2. Mineralization of F-GCSs and FT-GCSs.

(A) Alizarin red staining of F-GCSs and FT-GCSs after 0, 5, and 11 days of culture (Scale bar 100 µm). (B) Absorption (at 550 nm) was observed to determine the degree of mineralization on days 0, 5, and 11 in both groups. F-GCS, fresh gelatin-induced osteogenic cell sheet; FT-GCS, frozen-thawed gelatin-induced osteogenic cell sheet; GCS, gelatin-induced osteogenic cell sheet; OD, optical density. *, † $p < 0.05$, significant differences in F-GCSs and FT-GCSs, respectively, from that at day 0 (n = 3).
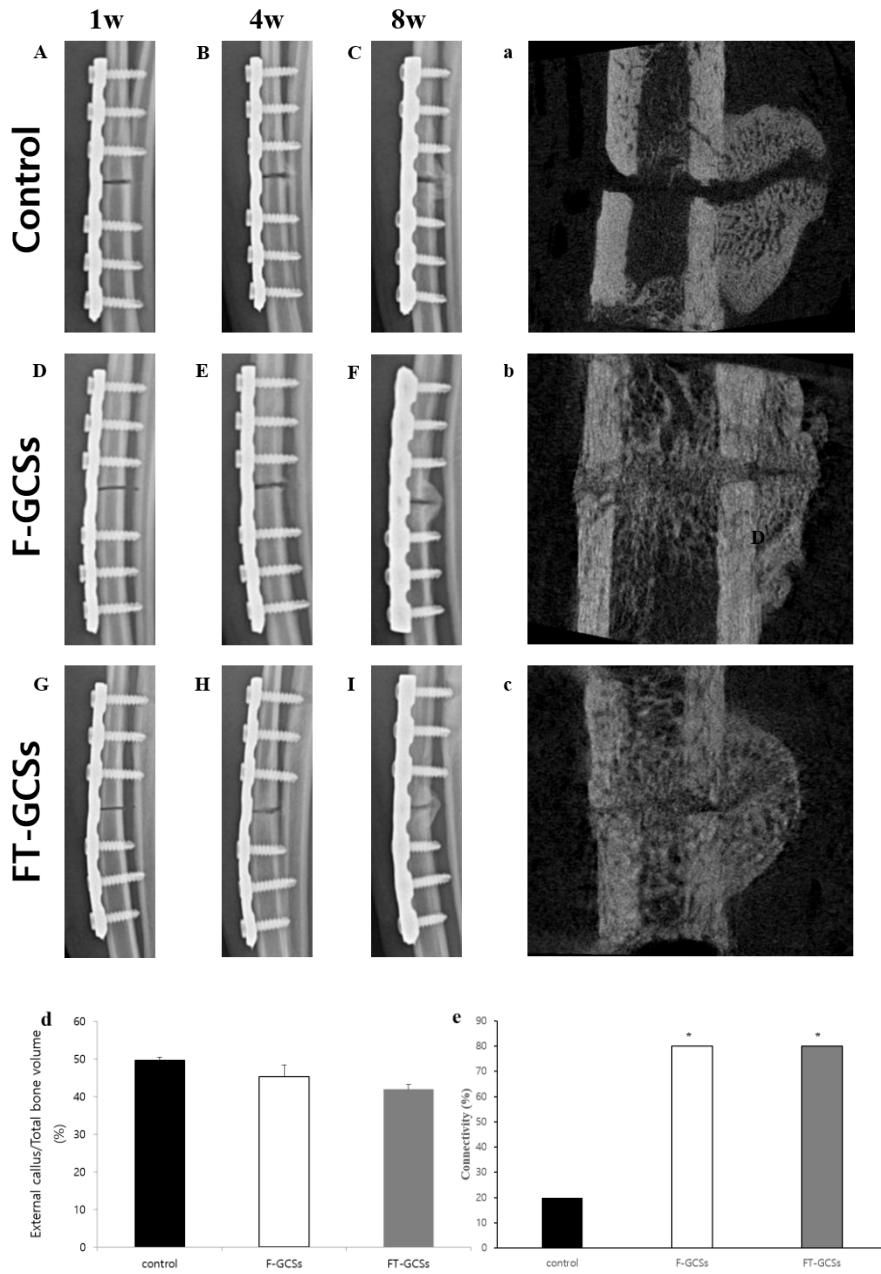
Fig. 2. 3. Radiographic & micro-computed tomography images.

(A-I) Radiographic examination showed that implants retained their position for the entire 8 weeks after surgery. (a-c) All groups showed the formation of large bony calluses but different percentages of bone connectivity. (d) There were no significant differences in the proportion of callus out of the total bone volume among the groups. (e) F-GCSs and FT-GCSs showed significantly better cortical bone connectivity than that of the control after 8 weeks of surgery. FT-GCS, frozen-thawed gelatin-induced osteogenic cell sheet; F-GCS, fresh gelatin-induced osteogenic cell sheet. * $p < 0.05$, significant difference from the control (n = 4).
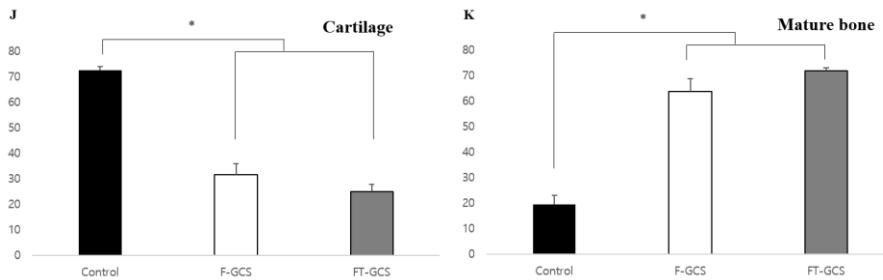
100 μm
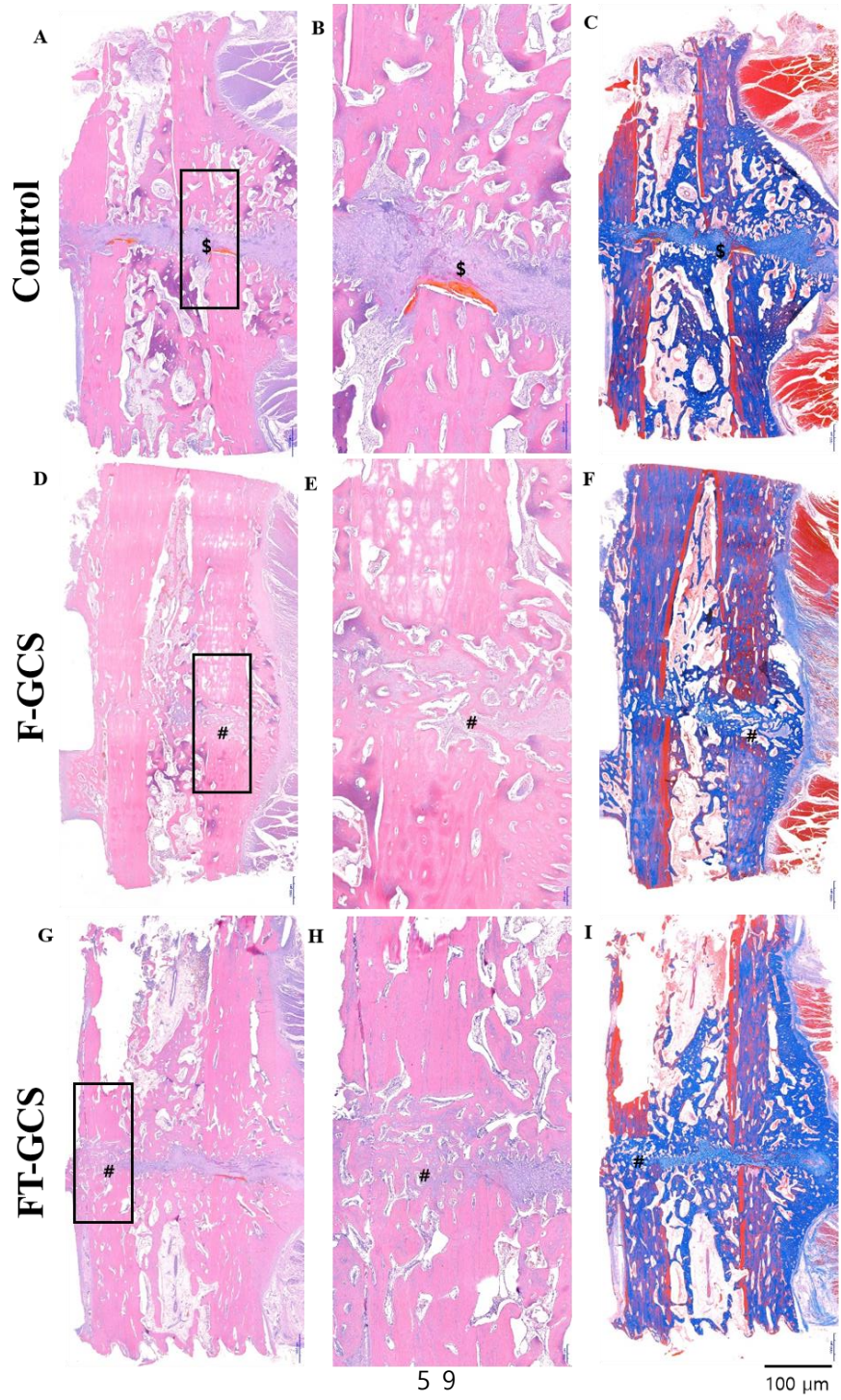
Fig. 2. 4. Histopathological staining of longitudinal sections of radius bone with mid-shaft transverse fracture after 8 weeks of healing with decalcification.

(A-C) Control group showed cartilage formation ($) without ossification at the fracture site. (D-I) F-GCSs and FT-GCSs groups showed fracture sites were well organized with both cartilage and mature bone (#) present. (B, E, H) are magnified images of A, D, and G, respectively. (J) The control treatment produced a significant ($p < 0.05$) presence of cartilage rather than mature bone (K); however, F-GCSs and FT-GCSs produced a significant ($p < 0.05$) presence of mature bone at the healing sites compared to that in the control. F-GCS, fresh gelatin-induced osteogenic cell sheet; FT-GCS, frozen-thawed gelatin-induced osteogenic cell sheet. * $p < 0.05$, significant difference from the control (Scale bar: 100 µm; n = 4).

GENERAL CONCLUSION

This study was conducted to investigate a method for promoting bone regeneration in fractures using osteogenic-induced stromal cell sheets.

The results of the experiments are as follows:

1. OCS expressed more osteogenic-related factors than UCS.

2. Using OCS, fracture sites might be stabilized by early bone healing and callus formation can be reduced.

3. UCS and OCS had different tissue healing effects. OCS could be used for bone healing.

4. There was no significant difference in osteogenic capability between F-

GCS and FT-GCS *in vitro*.

5. GCS was similarly effective for bone regeneration in the fresh as well as frozen and thawed states.

.

Overall, OCS can be clinically applied for early bone regeneration. In particular, OCS cultured with gelatin are more solid and osteogenic differentiated than OCS; even when frozen and stored, the bone regeneration effects of GCS can be expected. Therefore, FT-GCS could be used more conveniently than F-GCS.

REFERENCES

AE Rapp, R Bindl, A Heilmann, A Erbacher, I Müller, RE Brenner, A Ignatius. Systemic mesenchymal stem cell administration enhances bone formation in fracture repair but not load-induced bone formation. European Cells and Materials 2005; 29: 22-34.

Aenlle KK, Curtis KM, Roos BA, Howard GA. Hepatocyte Growth Factor and p38 Promote Osteogenic Differentiation of Human Mesenchymal Stem Cells. Molecular Endocrinology 2014; 28: 722-730.

Akahane M, Nakamura A, Ohgushi H, Shigematsu H, Dohi Y, Takakura Y. Osteogenic matrix sheet-cell transplantation using osteoblastic cell sheet resulted in bone formation without scaffold at an ectopic site. Journal of Tissue Engineering Regenerative Medicine 2008; 2: 196-201.

Akahane M, Shigematsu H, Tadokoro M, Ueha T, Matsumoto T, Tohma Y, Kido A, Imamura T, Tanaka Y. Scaffold-free cell sheet injection results in

bone formation. J Tissue Eng Regen Med 2010; 4: 404-411.

Aro HT, EY C. Bone-healing patterns affected by loading, fracture fragment stability, fracture type, and fracture site compression. Clin Orthop Relat Res 1993; 293: 8-17.

Bruder SP, Jaiswal N, Haynesworth SE. Growth kinetics, self-renewal, and the osteogenic potential of purified human mesenchymal stem cells during extensive subcultivation and following cryopreservation. J Cell Biochem 1997; 64: 278-294.

Chen G, Deng C, Li YP. TGF-beta and BMP signaling in osteoblast differentiation and bone formation. Int J Biol Sci 2012; 8: 272-288.

Chen L, Tredget EE, Wu PY, Wu Y. Paracrine factors of mesenchymal stem cells recruit macrophages and endothelial lineage cells and enhance wound healing. PLoS One 2008;   3: e1886.

Chinnadurai R, Garcia MA, Sakurai Y, Lam WA, Kirk AD, Galipeau J, Copland

IB. Actin cytoskeletal disruption following cryopreservation alters the biodistribution of human mesenchymal stromal cells in vivo. Stem Cell Reports 2014; 3: 60-72.

Chu Q, Wang Y, Fu X, Zhang S. Mechanism of in vitro differentiation of bone marrow stromal cells into neuron-like cells. J Huazhong Univ Sci Technolog Med Sci 2004; 24: 259-261.

Devine SM, Cobbs C, Jennings M, Bartholomew A, Hoffman R. Mesenchymal stem cells distribute to a wide range of tissues following systemic infusion into nonhuman primates. Blood 2003; 101: 2999-3001.

Dwek JR. The periosteum: what is it, where is it, and what mimics it in its absence? Skeletal Radiology 2010; 39: 319-323.

Egami M, Haraguchi Y, Shimizu T, Yamato M, Okano T. Latest status of the clinical and industrial applications of cell sheet engineering and regenerative medicine. Archives of pharmacal research 2014; 37: 96-106.

Endrigo GL Alves, Rogéria Serakides, Jankerle N Boeloni, Isabel R Rosado, Natália M Ocarino, Humberto P Oliveira, Alfredo M Góes, Cleuza MF Rezende. Comparison of the osteogenic potential of mesenchymal stem cells from the bone marrow and adipose tissue of young dogs. BMC Veterinary Research 2014; 10: 190.

Froelich K, Mickler J, Steusloff G, Technau A, Ramos Tirado M, Scherzed A, Hackenberg S, Radeloff A, Hagen R. Kleinsasser N. Chromosomal aberrations and deoxyribonucleic acid single-strand breaks in adipose-derived stem cells during long-term expansion in vitro. Cytotherapy 2013; 15: 767-781.

Geng W, Ma D, Yan X, Liu L, Cui J, Xie X, Li H, Chen, F. Engineering tubular bone using mesenchymal stem cell sheets and coral particles. Biochem Biophys Res Commun 2013; 433: 595-601.

Gregory CA, Gunn WG, Peister A, Prockop DJ. An Alizarin red-based assay of mineralization by adherent cells in culture: comparison with cetylpyridinium chloride extraction. Anal Biochem 2004; 329: 77-84.

Gu H, Xiong Z, Yin X, Li B, Mei N, Li G, Wang C. Bone regeneration in a
rabbit ulna defect model: use of allogeneic adipose-derivedstem cells
with low immunogenicity. Cell Tissue Res 2014; 358: 453-464.

Guo P, Zeng JJ, Zhou N. A Novel Experimental Study on the Fabrication and
Biological Characteristics of Canine Bone Marrow Mesenchymal Stem
Cells Sheet Using Vitamin C. Scanning 2015; 37: 42-48.

Hoch E, Schuh C, Hirth T, Tovar GE, Borchers K. Stiff gelatin hydrogels can
be photo-chemically synthesized from low viscous gelatin solutions
using molecularly functionalized gelatin with a high degree of
methacrylation. J Mater Sci Mater Med 2012; 23: 2607-2617.

Huang S, Xu L, Zhang Y, Sun Y, Li G. Systemic and Local Administration of
Allogeneic Bone Marrow-Derived Mesenchymal Stem Cells Promotes
Fracture Healing in Rats. Cell Transplant 2015; 24: 2643-2655.

Inagaki Y, Uematsu K, Akahane M, Morita Y, Ogawa M, Ueha T, Shimizu T,
Kura T, Kawate K,   Tanaka, Y. Osteogenic matrix cell sheet
transplantation enhances early tendon graft to bone tunnel healing in

rabbits. Biomed Res Int 2013; 842192.

Kassem M, Abdallah BM. Human bone-marrow-derived mesenchymal stem cells: biological characteristics and potential role in therapy of degenerative diseases. Cell Tissue Res 2008; 331: 157-163.

Kelm JM, Fussenegger M. Scaffold-free cell delivery for use in regenerative medicine. Adv Drug Deliv Rev 2010; 62: 753-764.

Kim AY, Kim Y, Lee SH, Yoon Y, Kim WH, Kweon OK. Effect of Gelatin on Osteogenic Cell Sheet Formation Using Canine Adipose-Derived Mesenchymal Stem Cells. Cell Transplant 2017; 26: 115-123.

Kim M, Kim Y, Lee S, Kuk M, Kim AY, Kim WH, Kweon OK. Comparison of viability and antioxidant capacity between canine adipose-derived mesenchymal stem cells and heme oxygenase-1-overexpressed cells after freeze-thawing. The Journal of Veterinary Medical Science 2016; 78: 619-625.

Komori T. Regulation of skeletal development by the Runx family of transcription factors. Journal of Cellular Biochemistry 2005; 95: 445-

453.

Komori T. Regulation of osteoblast differentiation by transcription factors. Journal of Cellular Biochemistry 2006; 99: 1233-1239.

Kotobuki N, Hirose M, Machida H, Katou Y, Muraki K, Takakura Y, Ohgushi H. Viability and osteogenic potential of cryopreserved human bone marrow-derived mesenchymal cells. Tissue Eng 2005; 11: 663-673.

Kudo O, Sabokbar A, Pocock A, Itonaga I, Fujikawa Y, Athanasou NA. Interleukin-6 and interleukin-11 support human osteoclast formation by a RANKL-independent mechanism. Bone 2003; 32: 1-7.

Kuk M, Kim Y, Lee SH, Kim WH, Kweon OK. Osteogenic Ability of Canine Adipose-Derived Mesenchymal Stromal Cell Sheets in Relation to Culture Time. Cell Transplant 2015; 25: 1415-1422.

Kura T, Akahane M, Shimizu T, Uchihara Y, Tohma Y, Morita Y, Koizumi M, Kawate K, Tanaka, Y. Use of Cryopreserved Osteogenic Matrix Cell

Sheets for Bone Reconstruction. Stem Cell Discovery 2016; 06: 13-23.

Lacey DC, Simmons PJ, Graves SE, Hamilton JA. Proinflammatory cytokines inhibit osteogenic differentiation from stem cells: implications for bone repair during inflammation. Osteoarthritis Cartilage 2009; 17: 735-742.

Lin YC, Grahovac T, Oh SJ, Ieraci M, Rubin JP, Marra KG. Evaluation of a multi-layer adipose-derived stem cell sheet in a full-thickness wound healing model. Acta Biomater 2013; 9: 5243-5250.

Livak KJ, Schmittgen TD. Analysis of relative gene expression data using real-time quantitative PCR and the 2(-Delta Delta C(T)) Method. Methods 2001; 25: 402-408.

Ma D, Ren L, Liu Y, Chen F, Zhang J, Xue Z, Mao T. Engineering scaffold-free bone tissue using bone marrow stromal cell sheets. J Orthop Res 2010; 28: 697-702.

Matsuda W, Haraguchi Y, Shimizu T, Miyoshi S, Umezawa A, Okano T.

Fabrication of three-dimensional tissues with multilayer mesenchymal stem cell sheets: overcoming the diffusion limit. Cardiovascular Revascularization Medicine 2008; 9: 110.

Matsuura K, Utoh R, Nagase K, Okano T. Cell sheet approach for tissue engineering and regenerative medicine. J Control Release 2014; 190: 228-239.

Melanie T, Heriburg H, Britta W, Wolfgang B, Thomas P, Georg S, Jochen ZRS, Michael J Raschke. Influence of antiTNF-alpha antibody treatment on fracture healing under chronic inflammation. BMC Musculoskeletal Disorders 2014; 15: 184.

Nakamura A, Akahane M, Shigematsu H, Tadokoro M, Morita Y, Ohgushi H, Dohi Y, Imamura T, Tanaka Y. Cell sheet transplantation of cultured mesenchymal stem cells enhances bone formation in a rat nonunion model. Bone 2010; 46: 418-424.

Napimoga MH, Demasi AP, Jarry CR, Ortega MC, de Araujo VC, Martinez EF.

In vitro evaluation of the biological effect of SOFAT on osteoblasts. Int Immunopharmacol 2015; 26: 378-383.

Okamoto M, Dohi Y, Ohgushi H, Shimaoka H, Ikeuchi M, Matsushima A, Yonemasu K, Hosoi H. Influence of the porosity of hydroxyapatite ceramics on in vitro and in vivo bone formation by cultured rat bone marrow stromal cells. J Mater Sci Mater Med 2006; 17: 327-336.

Pal R, Hanwate M, Totey SM. Effect of holding time, temperature and different parenteral solutions on viability and functionality of adult bone marrow-derived mesenchymal stem cells before transplantation. J Tissue Eng Regen Med 2008; 2: 436-444.

Palmqvist P, Persson E, Conaway HH, Lerner UH. IL-6, Leukemia Inhibitory Factor, and Oncostatin M Stimulate Bone Resorption and Regulate the Expression of Receptor Activator of NF- B Ligand, Osteoprotegerin, and Receptor Activator of NF- B in Mouse Calvariae. The Journal of Immunology 2002; 169: 3353-3362.

Parekkadan B, Milwid JM. Mesenchymal stem cells as therapeutics. Annu Rev

Biomed Eng 2010; 12: 87-117.

Pirraco RP, Obokata H, Iwata T, Marques AP, Tsuneda S, Yamato M, Reis RL, Okano, T. Development of osteogenic cell sheets for bone tissue engineering applications. Tissue Eng Part A 2011; 17: 1507-1515.

Rifas L, Weitzmann MN. A novel T cell cytokine, secreted osteoclastogenic factor of activated T cells, induces osteoclast formation in a RANKL-independent manner. Arthritis Rheum 2009; 60: 3324-3335.

Roemeling-van Rhijn M, de Klein A, Douben H, Pan Q, van der Laan LJ, Ijzermans JN, Betjes MG, Baan CC, Weimar W, Hoogduijn MJ. Culture expansion induces non-tumorigenic aneuploidy in adipose tissue-derived mesenchymal stromal cells. Cytotherapy 2013; 15: 1352-1361.

Rosellini E, Cristallini C, Barbani N, Vozzi G, Giusti P. Preparation and characterization of alginate/gelatin blend films for cardiac tissue engineering. J Biomed Mater Res A 2009; 91: 447-453.

Ryu HH, Lim JH, Byeon YE, Park JR, Seo MS, Lee YW, Kim WH, Kang KS, Kweon OK. Functional recovery and neural differentiation after transplantation of allogenic adipose-derived stem cells in a canine model of acute spinal cord injury. J Vet Sci 2009; 10: 273-284.

Sabat R, Grütz G, Warszawska K, Kirsch S, Witte E, Wolk K, Geginat J. Biology of interleukin-10. Cytokine & Growth Factor Reviews 2010; 21: 331-344.

Sanjabi S, Zenewicz LA, Kamanaka M, Flavell RA. Anti-inflammatory and pro-inflammatory roles of TGF-beta, IL-10, and IL-22 in immunity and autoimmunity. Curr Opin Pharmacol 2009; 9: 447-453.

Shimizu T, Akahane M, Morita Y, Omokawa S, Nakano K, Kira T, Onishi, T, Inagaki, Y, Okuda A. Kawate K, Tanaka, Y. The regeneration and augmentation of bone with injectable osteogenic cell sheet in a rat critical fracture healing model. Injury 2015; 46: 1457-1464.

Shimizu T, Akahane M, Ueha T, Kido A, Omokawa S, Kobata Y, Murata K, Kawate K, Tanaka Y.　Osteogenesis of cryopreserved osteogenic

matrix cell sheets. Cryobiology 2013; 66: 326-332.

Spurr EE, Wiggins NE, Marsden KA, Lowenthal RM, Ragg SJ. Cryopreserved human haematopoietic stem cells retain engraftment potential after extended (5-14 years) cryostorage. Cryobiology 2002; 44: 210-217.

Syed-Picard FN, Shah GA, Costello BJ, Sfeir C. Regeneration of periosteum by human bone marrow stromal cell sheets. J Oral Maxillofac Surg 2014; 72: 1078-1083.

Tobias KM, Johnston SA. Veterinary surgery: Small animal.St.Louis, MO: Elsevier; 2013; 565-571.

Uccelli A, Moretta L, Pistoia V. Mesenchymal stem cells in health and disease. Nat Rev Immunol 2008; 8: 726-736.

Uchihara Y, Akahane M, Shimizu T, Ueha T, Morita Y, Nakasaki S, Kura T, Tohma Y, Kido A, Kawate K, Tanaka, Y. Osteogenic Matrix Cell Sheets Facilitate Osteogenesis in Irradiated Rat Bone. Biomed Res Int,

2015; 629168.

Uchiyama H, Yamato M, Sasaki R, Okano T, Ogiuchi H. P.165 Bone regeneration using periosteum cell sheets harvested from temperature responsive culture dishes. Journal of Cranio-Maxillofacial Surgery Supplement 1 2006; 34: 174.

Uchiyama H, Yamato M, Sasaki R, Sekine H, Yang J, Ogiuchi H, Ando T, Okano T. In vivo 3D analysis with micro-computed tomography of rat calvaria bone regeneration using periosteal cell sheets fabricated on temperature-responsive culture dishes. J Tissue Eng Regen Med 2011; 5: 483-490.

Vaes BLT, Dechering KJ, Feijen A, Hendriks JMA, Lefèvre C, Mummery CL, Olijve W, Van ZEJJ, Steegenga WT. Comprehensive Microarray Analysis of Bone Morphogenetic Protein 2-Induced Osteoblast Differentiation Resulting in the Identification of Novel Markers for Bone Development. Journal of Bone and Mineral Research 2002; 17: 2106-2118.

Wang Z, Weng Y, Lu S, Zong C, Qiu J, Liu Y, Liu B. Osteoblastic mesenchymal stem cell sheet combined with Choukroun platelet-rich fibrin induces bone formation at an ectopic site. J Biomed Mater Res B Appl Biomater 2015; 103: 1204-1216.

Wei F, Qu C, Song T, Ding G, Fan Z, Liu D, Zhang C, Shi S, Wang S. Vitamin C treatment promotes mesenchymal stem cell sheet formation and tissue regeneration by elevating telomerase activity. J Cell Physiol 2012; 227: 3216-3224.

Wu SC, Chang WH, Dong GC, Chen KY, Chen YS, Yao CH. Cell adhesion and proliferation enhancement by gelatin nanofiber scaffolds. Journal of Bioactive and Compatible Polymers 2011; 26: 565-577.

Yang J, Yamato M, Shimizu T, Sekine H, Ohashi K, Kanzaki M, Ohki T, Nishida K, Okano T. Reconstruction of functional tissues with cell sheet engineering. Biomaterials 2007; 28: 5033-5043.

Yoon Y, Khan IU, Choi KU, Jung T, Jo K, Lee SH, Kim, WH, Kim DY, Kweon OK. Different Bone Healing Effects of Undifferentiated and

Osteogenic Differentiated Mesenchymal Stromal Cell Sheets in Canine Radial Fracture Model. Tissue Engineering and Regenerative Medicine 2017; 15:115-124.

Young DA, Gavrilov S, Pennington CJ, Nuttall RK, Edwards DR, Kitsis RN, Clark IM. Expression of metalloproteinases and inhibitors in the differentiation of P19CL6 cells into cardiac myocytes. Biochem Biophys Res Commun 2004; 322: 759-765.

Yu J, Tu YK, Tang YB, Cheng NC. Stemness and transdifferentiation of adipose-derived stem cells using L-ascorbic acid 2-phosphate-induced cell sheet formation. Biomaterials 2014; 35: 3516-3526.

국 문 초 록

개의 골절 모델에서 골분화를 유도한 중간엽

줄기세포 시트의 골재생 효과

지도교수 강 병 재

윤 용 석

서울대학교 대학원

수의학과 임상수의학 전공

골절 회복 과정에서의 불유합과 지연유합의 회복반응은
수의정형외과학에서 중요한 주제이다. 중간엽 유래의 줄기세포를
이용하여 제작한 세포시트가 골재생에 효과가 있다고 연구되어

있다. 또한 젤라틴을 이용하여 골분화 유도 줄기세포 시트 (GCS)를 제작하였을 때 골분화 유도 줄기세포 시트 (OCS)와 골재생능에 있어 큰 차이가 없음이 연구되었다.

두 파트로 구성된 본 연구의 첫 번째 실험에서 OCS 와 미분화세포시트 (UCS)의 골재생능에 대하여 비교하였다. 두 번째 실험에서는 젤라틴을 이용하여 배양한 골분화유도 줄기세포 시트의 신선한 상태와 동결시켰던 세포시트의 골재생 효과 차이를 확인하였다. 추가로 두 연구 모두 개 골절 모델에 적용하여 골 회복 반응을 평가하였다.

첫 번째 실험은 골절 회복에 있어서, 미분화 줄기세포 시트(UCS) 와 OCS의 골 재생 효과를 *in vitro* 와 *in vivo*상에서 비교한 것이다. 정량적 중합효소 연쇄반응 실험을 통하여 OCS의 경우 UCS에 비하여 골형성단백질7 (BMP7), 형성전화증식인자 (TGF-β), Runx2, 그리고 HGF가 상승된 것을 확인할 수 있었다. 반면 UCS의 경우 OCS에 비하여 시클로옥시게나이제-2 (COX-2), 인터류킨-6 (IL-6), 인터류킨-10 (IL-10) 종양괴사인자-알파 (TNF-α), 가 상승되어 있는 것을 확인할 수 있었다. 요골 골절 모델에서 각 줄기세포시트를 적용하였을 때, OCS를 적용한 군에서 가골의 양이 유의적으로 적게

80

형성된 것을 확인할 수 있었다. 조직염색을 통하여 OCS 군에서 성숙한 골화세포들을 확인할 수 있었다. 반면 UCS를 적용한 군에서는 섬유조직들의 유의적인 상승을 확인할 수 있었다. 따라서 OCS의 경우 초기 골재생을 통하여 골절부의 안정성이 증가되었고, 그로 인해 가골의 형성이 줄어든 것으로 생각된다. 또한 UCS와 OCS의 경우 조직재생에 있어 다른 효과가 있는 것으로 보이며, OCS는 골 재생을 기대할 수 있다.

OCS 제작 과정에 젤라틴을 이용하면 골분화 관련 인자들의 상승과 더 단단한 골분화 유도 줄기세포 시트를 제작할 수 있음이 연구되었다. 또한, OCS 와 GCS 의 경우 골분화 경로가 다름이 밝혀졌다. 첫 번째 실험 과정에서 골분화 줄기세포 시트를 배양하기 위하여 몇 일간의 시간이 소요되었기에, 이를 임상에 적용하기 용이한 방법으로 동결하여 보관했던 줄기세포 시트의 골재생 효능을 평가하였다.

두 번째 실험에서는 젤라틴을 이용하여 배양한 골분화 유도 줄기세포 시트 (F-GCS)와, 그것을 동결시켜 보관하였다가 녹인 골분화 유도 줄기세포 시트 (FT-GCS)의 골 재생 효과를 비교하였다. 실험은 크게 두 파트로, *in vitro* 에서 F-GCS 와 FT-

GCS 의 골분화 관련 평가, *in vivo* 에서는 요골 골절 모델의 비글견에게 적용하여 골재생 정도를 평가하였다. *In vitro* 실험, 정량적 중합효소 연쇄 반응 결과 F-GCS 와 FT-GCS 에서 골분화 관련 인자들의 수치들도 유의미적인 차이가 없었다. In vivo 결과에서는 가골이 세포시트를 적용해준 군에서 증가된 것을 확인할 수 있었고, 골절부분의 연결성은 통제군에 비하여 세포시트를 적용해준 군에서 유의미적으로 상승되었다. 조직 염색상에서 골절부의 피질골 사이 부분에서 F-GCS 군과 FT-GCS 군에서 성숙한 뼈의 양이 통제군에 비하여 유의미적으로 상승되어 있는 것을 확인할 수 있었고, 두 군의 차이는 없었다. 따라서 젤라틴을 이용하여 배양한 골분화유도 줄기세포 시트의 경우, 신선한 상태에서 바로 사용하는 것과 동결 후 냉동 과정을 거쳐서 사용하여도 골재생에 비슷한 정도의 효과를 보인다.

결론적으로 골분화 유도 줄기세포시트의 경우, 빠른 골재생을 기대할 때 임상적으로 적용이 가능하다. 특히 젤라틴을 이용하여 배양한 골분화 유도 줄기세포 시트의 경우에는 골분화 유도 줄기세포시트에 비하여 단단하고 골분화가 더 많이 진행되며,

동결하여 보관하다가 사용하더라도 골분화 유도 줄기세포 시트의

골재생 효과를 기대할 수 있다.